Synthesis of A New Perylene Derivative Ligand Potential for DNA Binding

Safieh Fotovatnia

Submitted to the
Institute of Graduate Studies and Research
in partial fulfillment of the requirement for the Degree of

Master of Science
in
Chemistry

Eastern Mediterranean University
February 2015
Gazimağusa, North Cyprus

Approval of the Institute of Graduate Studies and Research

Prof. Dr. Serhan Çiftçioğlu
Acting Director

I certify that this thesis satisfies the requirements as a thesis for the degree of Master of Science in Chemistry.

Prof. Dr. Mustafa Halilsoy
Chair, Department of Chemistry

We certify that we have read this thesis and that in our opinion it is fully adequate in scope and quality as a thesis for the degree of Master of Science in Chemistry.

Prof. Dr. Huriye İcil
Supervisor

Examining Committee

1. Prof. Dr. Huriye İcil _____

2. Asst. Prof. Dr. Jagadeesh B. Bodapati _____

3. Asst. Prof. Dr. Hürmüs Refiker _____

ABSTRACT

The main aim of this project was the synthesis of a novel perylene compound, named, N-(1-dehydroabietyl)-3,4,9,10-perylenetetracarboxylic-3,4-anhydride-9,10-imide (ABPMI), from N-N'-di(1-dehydroabietyl)perylene-3,4,9,10-bis(dicarboxymide) (ABPDI) for future DNA binding studies. The product was characterized by FT-IR, UV-vis and emission spectrometry. The optical and photophysical properties have been investigated in detail.

ABPMI showed moderate solubility in some common organic solvents like chloroform, DMF and methanol. In the UV-vis absorption spectra of ABPMI in chloroform and methanol three characteristic peaks have been observed at 439, 469 and 517 nm, respectively (with small red shift in methanol). In absorption spectrum of ABPMI in DMF, three peaks have been achieved at 439, 465 and 518 nm, with the reversal intensity between 0→0 and 0→1 transition. In emission spectra of ABPMI in chloroform, DMF and methanol, excimer-like peaks have been observed. The optical band gap energy of ABPMI has been calculated as 1.984 eV.

The synthesized compound is promising as a potential ligand for future DNA binding studies.

Keywords: Perylene diimide, Perylene monoimide, Perylene dye

ÖZ

Bu projenin temel amacı, N-(1-dehidroabietil)-3,4,9,10-perilen tetrakarboksilik-3,4-anhidrit-9,10-imid (ABPMI) adlı yeni bir perilen bileşiğinin, N,N'-di(1-dehidroabietil) perilen-3,4,9,10-bis(dikarboksimid) (ABPDI) adlı perilen diimidden gelecekte DNA'ya bağlanma çalışmaları için sentezlenmiştir. Sentezlenen madde, FT-IR, UV-Vis ve emisyon ölçümleri ile karakterize edilmiştir. Optik ve fotofiziksel özellikleri detaylı olarak incelenmiştir.

ABPMI, kloroform, DMF ve metanol gibi bazı genel organik çözücüler içinde orta seviyede çözünürlük göstermiştir. ABPMI'nın kloroform ve metanol çözücülerindeki UV-vis absorpsiyon spektrumlarında sırasıyla 439, 469 ve 517 nm'de üç karakteristik pik (metanolda küçük kırmızı kayma) gözlenmiştir. ABPMI'ın DMF çözeltisindeki UV-vis absorpsiyon spektrumunda 0→0 ve 0→1 geçişlerinde ters şiddette üç absorpsiyon piki 439, 465, ve 518 nm'de elde edilmiştir. ABPMI'nın kloroform, DMF ve metanol çözücülerindeki emisyon spektrumlarında ekzimer-benzeri pikler gözlenmiştir. ABPMI'ın optik band enerjisi aralığı 1.98 eV olarak hesaplanmıştır.

Sentezlenen madde gelecekte DNA'ya bağlanma çalışmaları için potansiyel bir ligand olarak umut vericidir.

Anahtar Kelimeler: Perilen diimid, Perilen monoimid, Perilen boya

To my lovely family and my lovely professor

Prof. Dr. Huriye Icil

ACKNOWLEDGMENT

At first, I would like to say a special thanks to my patient supervisor Prof. Dr. Huriye Icil for her efforts and guidance through my master thesis. She always motivated me and gave me high energy during both my life and my research.

Secondly, I'm thankful from Organic Chemistry group members in Eastern Mediterranean University, specially Dr. Duygu Uzun because of her extreme helps and her efforts during the process of my thesis.

Last but not the least, I'm pleased to express my special thanks to my honorable family for their supports through my life and my study despite various difficulties.

TABLE OF CONTENTS

LIST OF TABLES

LIST OF FIGURES

LIST OF ILLUSTRATIONS

LIST OF ABBREVIATIONS/SYMBOLS

Å	Armstrong
cm	Centimeter
^0C	Degrees Celcius
$\Delta\bar{\upsilon}_{1/2}$	Half-width of the selected Absorption
ε_{max}	Maximum Extinction Coefficient
E_s	Singlet Energy
f	Oscillator strength
λ_{max}	Absorption wavelength maximum
δ	Chemical shift (ppm)
τ_0	Theoretical Radiative Lifetime
τ_f	Fluorescence Lifetime
Φ_f	Fluorescence Quantum Yield
nm	Nanometer
$CHCl_3$	Chloroform
CHL	Chloroform
DMF	N,N'-dimethylformamide
DNA	Deoxyribonucleic acid
FT-IR	Fourier Transform Infrared Spectroscopy
HCl	Hydrochloric Acid
KBr	Potassium Bromide
k_f	Theoretical Fluorescence Rate Constant
KOH	Potassium hydroxide
M	Molar Concentration

MeOH	Methanol
NaOH	Sodium hydroxide
RNA	Ribonucleic Acid
UV-vis	Ultraviolet Visible Absorption Spectroscopy

Chapter 1

INTRODUCTION

Perylene is one of the members of rylenes with an extended aromatic core which consists of naphthalene unit connections. This highly versatile chromophoric compound was discovered in 1913 by Kardos. Perylene derivatives possess a strong potential into the broad scope of applications like photovoltaic devices, solar cells, anti-cancer agents, dying the live cells, and also sensors based on pH. These applications are due to their outstanding features such as chemical, thermal and photochemical stabilities. Large molar absorption coefficient, high fluorescent quantum yield (FQY) and emition spectra above 500 nm, are some of their properties. This compound is a chromophore responsible for the color of substances. So, they are used in some fields as functional dyes[1].

Perylene tetracaerboxylic dianhydride (PTCDA) is an insoluble compound because of, its big aromatic core. The extended aromatic core of perylne derivatives leads to stacking interactions in solution state and also solid state. The result gives poor solubility. This solubility problem gives some applications such as organic pigments or vat dyes in car paintings and nail polish. A replacement of Oxygene atoms by Nitrogene atomes can improve its solubility. Nevertheless, in order to overcome its solubility obstacle, some organic substitutions introduce into the aromatic moiety or Nitrogene atoms. So, it can undergo different substitutions and therefore gives a wide range of perylene derivatives. In these molecules, nitrogen atoms belong to imides

group are connected to the long alkyl chains or tert-butyl groups (swallow-tail substituents). Another type of perylene derivatives can obtaine via introduce of some different alkyl side chains on both carboxylic scaffold (bay-positions) and nitrogene atoms (N-substitutions). The aggregation and solubility properties of perylene derivatives could be controlled by both substitutions. The photho-stability and color features, respectively, are governed by the substitution at the imide positions (N-substitution) and on the bay area (bay-substitution) of the perylene structure [2].

As mentined before [2], Perylene dyes have π-π stacking feature. So, they are suitable to bind DNA by stacking interactions and can act as anti-cancer agents. One approach to this goal is designe and synthesis of perylene derivatives with the role of telomerase inhibitor. It's possible by use of DNA structures [3].

Deoxyribonucleic acid (DNA), as the genetic material, was discovered in 1944. DNA has been known as a biomolecule which has the important role of coding the genetic information in all live creatures. It can apply in the targeted cancer treatment by use of its G - quadruplex structure. There is a specific short and non-coding tandem sequence at each end of human chromosome which named telomere. This sequence consists of TTAGGG sequence (Thymine- Thymine, Adenine, Guanine, Guanine, Guanine. Telomerase enzyme is responsible for the synthesis of telomeric DNA by enhancing TTAGG repeated units. Perylene derivatves as anticancer agents can performe π-π stacking interactions and also electrostatic interactions with telomere region of DNA and change it to G-quadruplex structure. The G - quadroplex structure is inaccessible for telomerase enzyme. Thus, it can inhibit the telomerase activity [4]

It’s worth noting that, the amount of telomerase is less in normal cells and more in tumor cells [5]

In the present research, we focused on the synthesis and characterization of an effective perylene material based ligand, N-(1-dehydroabietyl) – 3, 4, 9, 10-perylenetetracarboxylic-3, 4-anhydride-9, 10-imide (ABPMI). The compound was characterized by FTIR, UV-vis and emission spectrometry.

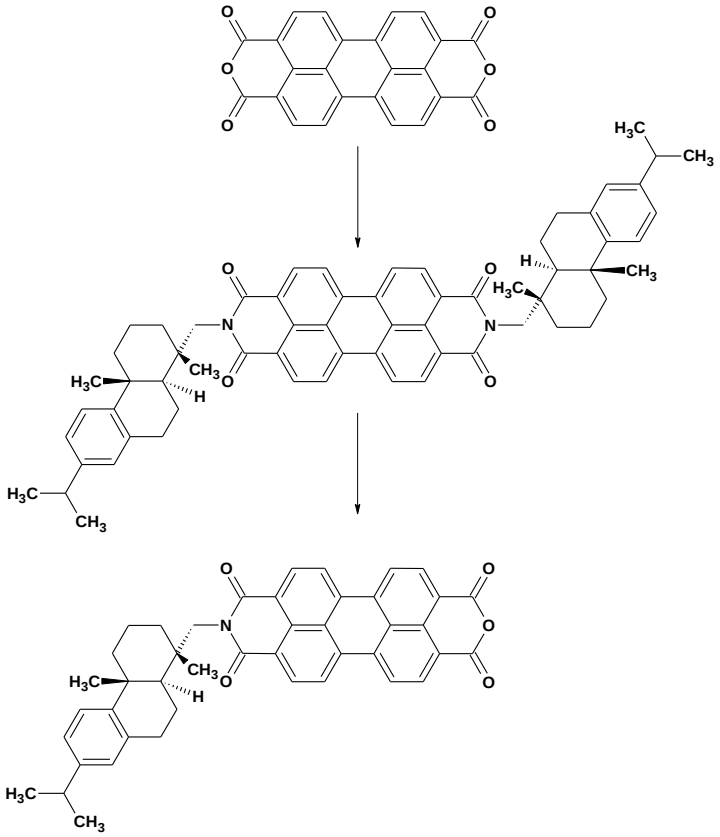

Schem 1.1: Synthesis of N-(1-dehydroabietyl) - 3, 4, 9, 10-perylenetetracarboxylic-3, 4-anhydride-9, 10-imide (ABPMI)

Chapter 2

THEORETICAL

2.1 The Structural Properties of DNA

DNA or Deoxyribonucleic acid was discovered as the essential genetic matter in 1944. The illustration of DNA structure, as a double helix, was described in 1953 (Figure 2.1) [6].

Figure 2.1: DNA

DNA is a genetic material which encodes and stores the genetic information. DNA has two major functions like transcription and replication. Most of DNA molecules are biopolymers. They are double stranded helix or two tall biopolymers made of simple units or monomers named Nucleotides. Each nucleotide unit has nucleobases which consists of nitrogen with the name of Guanine (G), Adenine (A), Cytosine (C), Thymine (T), a backbone including alternative pentose sugar or deoxyribose (5

carbon) and a phosphate group derived from phosphoric acid. In the nucleotide structure, nucleobases are attached to the pentose [6].

There are two categories of nucleobases based on number of members:

1. Purine is composed of 9 membered with a duplex-ring structure or heterocyclic with Adenine and Guanine bases.
2. Pyrimidine consists of 6 membered single-string construction with Cytosine and Thymine [6].

The genetic information replication happens, while two strings are separate and oriented in opposite directions. Thus, it has been deduced that both of them drive in antiparallel orientations to each other and produce anti-parallel strands. In other words, one construction starts with three primers (3′) and another starts by five primers (5′). In this backbone, one of four nucleobases is attached to the sugar and this sequence encodes the genetic information through the DNA [6].

DNA as a tall biopolymer made of monomer repeated unities named nucleotides. The double coils of DNA stabilizes by two distinct forces:

1. Hydrogen bondings among nucleotides.
2. Stacking π-π interactions between aromatic nucleobases [6].

Twin helix strands can form the DNA backbone. On the other hand, other twin helical strings may have some spaces. These spaces have been called grooves. They are not equal and therefore they don't have different sizes. The DNA grooves are two kinds:

1. Major grooves with 220 Å wide.

2. Minor grooves with 120 Å wide (Figure 2.2) [6].

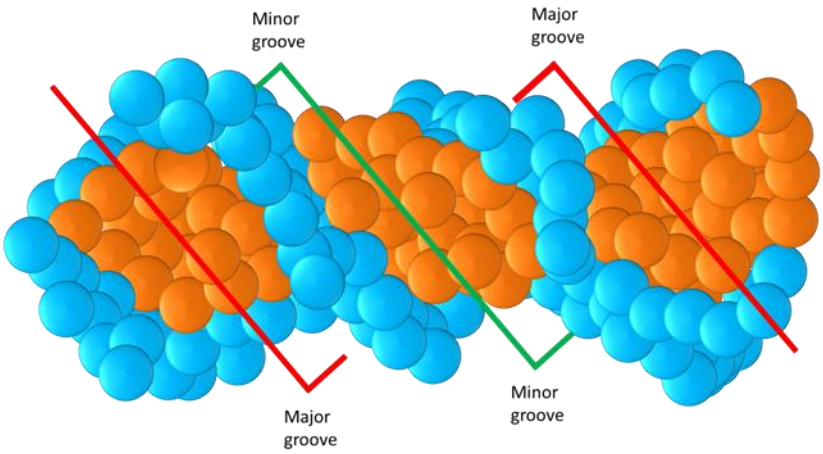

Figure 2.2: Major Grooves and Minor Grooves

The major grooves show the maximum edge rather than major grooves, so the major grooves are more accessible than minor grooves. In a twin helical DNA strand, each kind of nocleobase on the opposite string can connect to its supplement base on the other opposite strand. In other words, purine forms hydrogen boning to pyrimidine with two hydrogen bonding between A and T and three hydrogen bonding among G and C. This function is Supplementary Base Coupling. The hydrogen linkages are simply capable to re-break and re-connect. It is due to their non-covalent bond property [6].

The classification of the DNA structure is based on some items like sequence of the DNA molecule and its environment. The common classified structures of DNA are A-DNA, B-DNA (Figure 2.3) and Z-DNA. A-DNA and B-DNA are right handed strings with the same number of pairs of bases at every turn of helix. A-DNA has a stunted and broad structure equal to 2.2 nm in diameter and B-DNA has a high and slim structure with the size of 2 nm in diameter. The other sort of DNA structure is Z-DNA with a left handed, narrow and long structure with 12 bases per each turn of

the complex helices. In Z-DNA structure, the groove sare completely opposite A-DNA. [7].

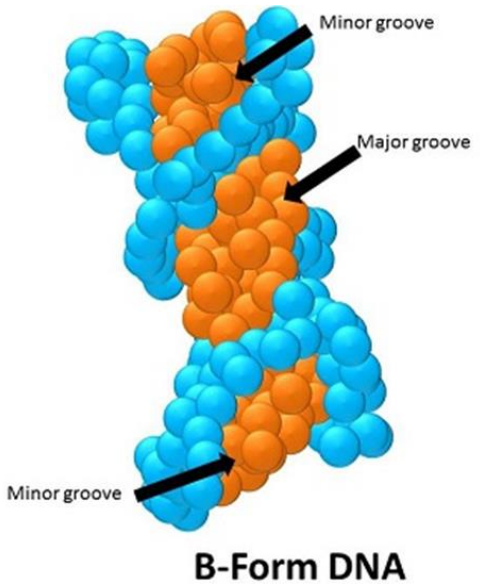

Figure 2.3: B-DNA

2.1.1 G-Quadruplex Structure

A chromosome is a single-stranded structure of DNA. There are unique areas at the end part of every chromosome. They are long Guanine-rich and single strands. This region is consists of thousands of repeated nucleotides to form of Thymine, Thymine, Adenine, Guanine, Guanine, Guanine (TTAGGG) sequences that are called Telomere.

The significant responsibility of these noncoding regions is letting the telomerase enzyme to copy or enhance the terminal end of chromosomes. The other role of these unique regions is maintenance and preventing of DNA terminus from DNA repairing and damages.

Sequences are liable to stabilize chromosomal DNA by two ways:

1. π-π stacking interactions of Guanine bases to form a structure with stack of four based module. These G-bases stack on each other and form a stable tetragonal superficial disc that is named G-quadruplex structure. This unusual structure possesses a metal ion (sodium or potassium) in the center of the quadruplex structure (Figure 2.4).

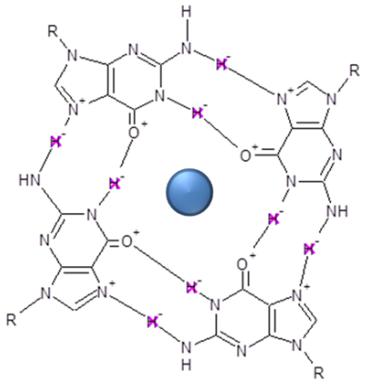

Figure 2.4: G-quadruplex Structure

2. Single strings of DNA are fixed by use of some binding proteins which are made up of telomere, in the form of a tall circle. This structure appears, as a result of rotation of a single strand of DNA [8].

As mentioned before [8], The four Guanine bases of G-quadruplex are linked to each other via H-H interactions (Hoogsteene hydrogen bonding). It can organize a flat four square structure called G-tetrad or G4-DNA. The G-tetrad structure is stabilized by sodium or potassium ion which is placed at the center of the structure. It is inaccessible for telomerase enzyme. The types of G-quadruplex depend on their sequence parts. It leads to the formation of tetrad structure which is described in the part below:

1. Intra-molecular: This structure formed by just one strand. There are four distinct lines of Guanine nucleobases in the single string which leads to stabilized quadruple skeleton.
2. Bimolecular: Longer sequences on two distinct strings are involved in this class. This subsequence is made of two continual rows of two or more than two Guanine nucleobases. Theses guanine areas are isolated by one or more different nucleobases.
3. Tetra molecular: These are short subsequences, composed of a single continuous line of three or more Guanine bases on four separate strands.

According to the arrangement of individual G-rich regions on intra-molecular or bimolecular structures, the diverse of loop configuration in Quadruple structure gives two the diversity of topology:

1. Parallel: The 5′ and 3′ terminal ends of all strands are similar.
2. Antiparallel: The 5′ and 3′terminus ends of several strands are different from another strands [9].

The normal somatic cells have 20% telomerase. However, some genetic mutations damage the DNA that may lead to impacts on telomerase activity. This is because of the increase of its activity and amount of the enzyme. This can be due to the environment. This means that the amount and activity of it changes to 85% and consequently causes very high cellular growth and generates the tumor cells. So, the telomerase and its activity can change to an anticancer target in chemotherapy. This method is possible by generating the inaccessible G-quadruple structure for telomerase and thus, inhibits more activity of the enzyme [10].

2.2 Binding organic Molecules to Particular DNA Sequences

DNA binding site are the places in DNA, which are suitable for binding interactions. These are recognized as short sequences of DNA which can bound to one or more protein complex. Specific DNA binding sites have been developed via protein binding molecules and other binding molecules. The connection between specific DNA binding sites and binding molecules or proteins starts, when the unique protein binds to these DNA sites. This manner can be simulated by small molecules. It means that they can bind to these sites of DNA and adjust, active or inhibit the DNA behavior related to the noted sequence. So these selective DNA binders can act as drugs to improve DNA functions.

The specific interactions of medicines to DNA are consist of two major reactions:

1. Irreversible covalent binding interactions of DNA with covalent binders like Cis-Diamminedichloroplatinium (Cis-platine) lead to the prevention of process of DNA and the cell dies (Figure 2.5).

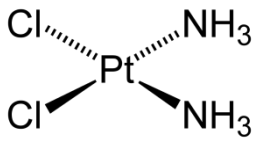

Figure 2.5: Cis-Platine: A Covalent Binder

2. Noncovalent binding interactions of DNA with non-covalent binders. They are known as minor groove binders, such as Mithramycin, Distamycine and other crescent form binder and intercalates like Nogalamycine, Menogaril (Figure 5) with a superficial cyclic group including O, N, F, S atoms [11,12].

2.2.1 Organic Molecule-DNA Building Blocks

In today's modern life, fighting with cancer has resulted in a wide range of researches about cancer. As a summary, there are two drug categories:

3. Antitelomerse.
4. Antitelomerase.

It's worth nothing that, telomere consists of two components; one hTRE (protein reverse transcriptase part) and hTR (RNA part). There are some extended numbers of drugs in each of these groups which are briefly mentioned here:

1. Drugs which target the hTERT are composed of Nucleoside, or Non-nucleoside inhibitors, Ribozymes.
2. Drugs by targeting the hTR include Antisense oligonucleotides.
3. Adjusting the telomerase Mechanisms at two both levels: the Transcriptional or Post-transcriptional. These drugs are well known by the name of their inhibition levels.
4. Compound targeting telomeres and associated proteins consists of G-Quadruple formation and interactive drugs and common cyto-toxic compounds.

Among these compounds, the G-Quadruple reactants are highly significant in target chemotherapy. As an example, Perylene dyes play blocker role for DNA. This function is usable in the pharmacology, pharmacy or targeted cancer therapy. For example, a class of DNA building blocker was synthesized (Figure 2.6). It has a perylene core, two N-cyclic swallow tails and one heterocyclic side arm. This compound binds to damaged DNA. The response of this connection to compound is the forming of inaccessible superficial tetragonal disc (G-quadruplex). This structure

was an obstacle against telomerase and therefore blocks its path. In consequence, telomerase enzyme will be stopped. Thus, it was formerly accepted as a compound killer for tumor cells in cancer [13,14].

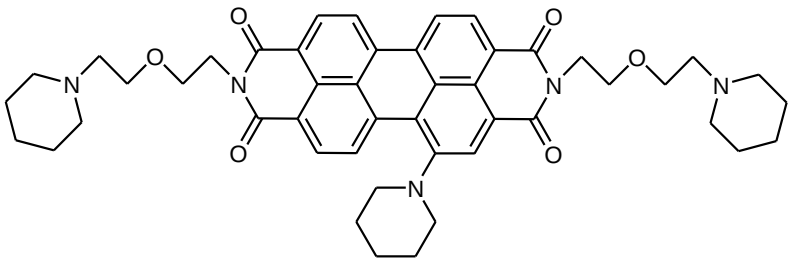

Figure 2.6: PBI as a Building Block

2.2.2 Ligands which bind DNA G-Quadruple Structure

G-Quadruple, as a specific target for chemotherapy is under intense investigation. There are different ligands that can specifically bind to this unusual secondary DNA structure. They lead to specific targeting in cancer. There are a wide range of small molecules which target G-Quadruplex and give cancer prevention. For instance:

1. Inactivating the promoter site and inhibition of oncogene expression. Porphyrin (TMPyPM4) is one of the cell permeable agents. It has distinct behavior with G-quadruplex structures, gene deactivation and thus nonspecific toxicity.
2. Telomerase inhibition by G-quadruplex structure formation. This category has three common members. The first one is 2, 6-Diamido Anthraquinones (BSU105), with high cytotoxicity, same as tumor cells. This is a DNA interactive ligand with an acceptable selectivity to triplex DNA and weak affinity to duplex DNA. This ligand will bind to G-Quadruple and stabilize it and form intra-molecular G-Quadruple structure. Consequently, they inhibit telomerase enzyme. The second one is Cationic porphyrin which is under

intense attention in photodynamic therapy in cancer. This application is due to their capability of high aggregations in tumor cells. The superficial aromatic part of the theme is suitable to assemble on G-tetrad and G-Quadruple formation. Tetra (N-methyl, 4-pyridyle)-porphine can bind to G-Quadruple, and then stabilize two kinds of anti-parallel and parallel G-Quadruple. The last one is perylene category. The important memember in perylene group is PIPER. It possesses two positively charged imide substitution (Figure 2.7). This remarkable compound has unique selectivity and affinity to G-Quadruple. These manners, respectively, are due to their big aromatic core and the positive charge chains at the two imide groups of the PIPER [15].

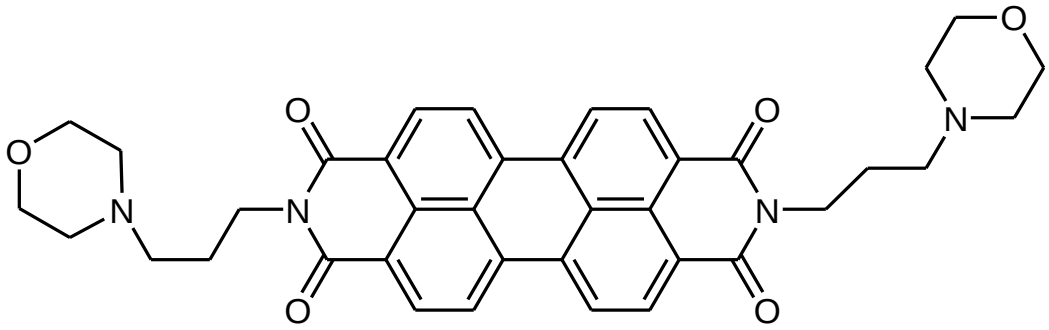

Figure 2.7: PIPER

2.3 An Overview on Perylene Dyes

Rylenes are remarkable classes of the hydrocarbon category. They are chemical compounds include of naphthalene linkages (Figure 2.8).

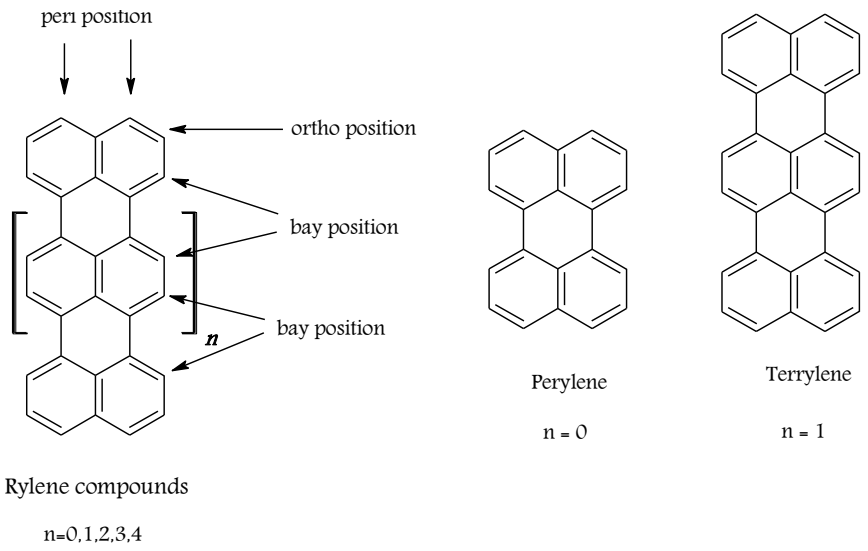

Figure 2.8: Ryelene Dyes

Chromophore belong to rylenes illustrate the unique property such as considerable thermal stability. This feature is because of its very high energy, which is responsible for resonance stabilization. At the same time, it gives excellent chemical stability as well. It can lead to light fastness in visible region. Perylene is one of the most useful and remarkable rylenes which is used in a broad scope of applications (Figure 2.9).

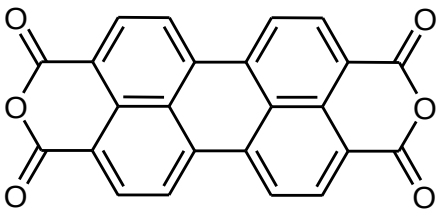

Figure 2.9: Perylene Tetracarboxylic Dianhydride

Perylene Tetracarboxylic Dianhydride is a polycyclic aromatic molecule composed of 5 rings connected to each other by peri-positions. It was founded in the tar belonging to coal. Moreover, it was discovered by Roland Scholl in 1910 by synthesis way of oxidation pairing of naphthalene unity in the presence of anhydrous aluminum tri-chloride [16]. They are extremely under regard due to their outstanding features. For instance, they have high absorption spectra because of its large molar

absorptivity. In addition, emission light is more than 500 nm because of its strong fluorescent quantum yield (FQY). They also have low solubility because of π-π stacking interactions and charge transport exclusions [17-18].

It's worth nothing that, addition of each naphthalene unit leads to increase the red shift in absorption spectra as well as in the molar absorption coefficient. Recently noted properties are highly regarded and under investigations to apply these functional dyes in photovoltaic devices, pharmacotherapy, industry, biology, pharmaceuticals and dye lasers. [19].

2.3.1. General Structural Properties

Perylene derivatives are insoluble due to their very big aromatic core which makes them suitable for π-π stacking interactions of aromatic moieties in solutions (π-orbitals overlap with adjacent molecules) and give self-aggregation. This special property of perylene dyes leads to a useful advantage as vat dyes [20-29]. For instance, they can play a role as a pigment in car painting. It is because of the presence of auxo-chrome groups responsible for their electronic and optical features. So, they can used as colorants due to their color. The limited solubility of these compounds is a serious drawback for utilization of them in some important applications. It has impact on fluorescent property of the chromophore by quenching phenomena. [30].

2.3.2 Structural Advantages of Perylene Dyes for DNA Binding

Perylene derivatives have an extended aromatic core. They can possess polar bay substitutions, imide substitutions or both of them. According to their structures, the large aromatic core is available in the center of them and it is suitable for π-π stacking interactions on the G4-DNA (G tetrad or G-Quadruple) of the terminal part

of DNA. On the other hand, the negative or positive charged side chains are at the imides section or at the bay area of the dye. Additionally, these positive charged chains leads to electrostatic interactions with phosphate groups of DNA groove. On the basis of their structures, the aggregation and solubility properties of perylene dervatives could be controlled by both substitutions, at imide section and the bay region. The photho-stability and color features, respectively are governed by the substitution at the imide positions (N-substitution) and at the bay zone (bay-substitution) of the perylene core. It's worth nothing that, the electrostatic-interactions causes the forming and stabilizing of the unusual G-Quadruple structures. It has an influence on G-Quadruplex topology. From the scientific point of view, the space of the hydrophilic side chains from the related aromatic core and their numbers, has an effect on induce, stabilize and finally, formation of the G-Quadruplex DNA. Thus, it can inhibit telomerase at the end of its interactions. The hydrophobic aromatic core leads to aggregations. Hydrophilic side chain can help to improve the solubility and give moderate water solubility (Figure 2.10). Briefly, some perylene derivatives have perfect selectivity and good affinity to G-Quadruple structure of DNA. With regard to all noted structures of perylene derivatives, substitution to the imides group gives a batho-chromic shift in the UV-V spectrum [31].

2.3.3 Functionalization of Perylene Chromophore for Binding DNA

As already mentioned [32], there are some functionalization reactions on the perylene moiety to get perylene derivatives. They are listed by name of Perylene Diimide derivatives, Perylene Mono imide derivatives, Perylene Tetra ester derivatives, Perylene Diester Dianhydride derivatives and etc. The starting substance to produce perylene diimide (PDI) is perylene-3, 4, 9, 10- (dicarboximide) or

perylene tetracarboxylic acid dianhydride (PTCA). The anhydride group changes to the imide group with dehydration reaction and consequently gives perylene Bis imide (PBI). For instance, Langhals synthesized it by use of imidazole in the role of base and zinc acetate in the function of catalyst. The reaction was under an initial alcoholic condition. In order to overcome the serious solubility problem of PBIs, the substituting by polar side chains is common. There are two positions for functionalization: One at the imide groups and another on the bay area of the perylene moieties. Other examples of perylene are Perylene Tetra Esters (PTEs), Peryelne Mono Diester (PIEs) and Peryleme mono imide mono anhydride (PMI). They have a broad scope of applications in industry, pharmacy and targeted chemotherapy. As a conclusion in perylene category, Perylene Bis imide and Perylene Tetraesters have good electron withdrawing property. They have the ability to form π-π stacking reaction in both solution and solid state. In the case of Perylene diester, a combination of these functional groups in one unique molecule gives good solubility. As a comparison, ester group is a better selection for attacking group rather than anhydride in perylene mono anhydride and mono imide. It plays a intermediate role in the way of unsymmetrical perylene dyes procedure. Perylene dyes are sensitive to change of environment's pH and will be deactivated at the high amount of pH. [34].

Consequently, perylene dyes are a class of versatile compounds with a broad scope of applications in pharmacology and targeted cancer therapy. Their significant applications are anticancer agent, pH sensor and industry applications like in solar cells and fluorescent dye chemistry. As anticancer agent, they can bind to a telomere sequence of DNA, leads to the formation of G-Quadruplex (G-tetrad) structure and

finally, inhibit telomerase activity. In addition, these compounds reduce and stabilize G-tetrad with good selectivity and moderate affinity. Besides this application, they are also used as a tracer inside the body by injection. They are fluorescent chromophore and they are nontoxic. They can also act as an on-off switch in different pH media. Therefore, they can apply as a pH sensor in vivo.

Chapter 3

EXPERIMENTAL

3.1 Materials and Characterization Methods

The perylene tetracarboxylic dianhydride and Potassium hydroxide were bought from Sigma Aldrich company and used without any purification. Dichloromethanol and Isopropanol were purchased from Merck. Chloroform and methanol were distilled based on standard procedure [35].

3.2 Instrumentation

FT-IR Spectroscopy:

Mattson Sattelite FT-IR spectrometer was used for structural characterizations of the synthesized compounds.

UV-vis spectroscopy:

Varian Cary-100 spectrophotometer was used in order to measure ultraviolet absorption spectra in solution.

Emission spectrometery:

Varian cary Eclipse spectrophotometer was used for fluorescence spectra.

3.3 Methods of Synthesis

The main target of this strategy is to design and synthesize N-(1-dehydroabietyl) - 3, 4, 9, 10-perylenetetracarboxylic-3, 4-anhydride-9, 10-imide (ABPMI) from N-N′-di (1-dehydroabietyl) perylene 3, 4, 9, 10-bis (Dicarboxymide) (ABPDI).

N-(1-dehydroabietyl) - 3, 4, 9, 10-perylenetetracarboxylic-3, 4-anhydride-9, 10-imide (ABPDI) was successfuly synthesized and purified according to published procedure (Scheme 3.1) [36].

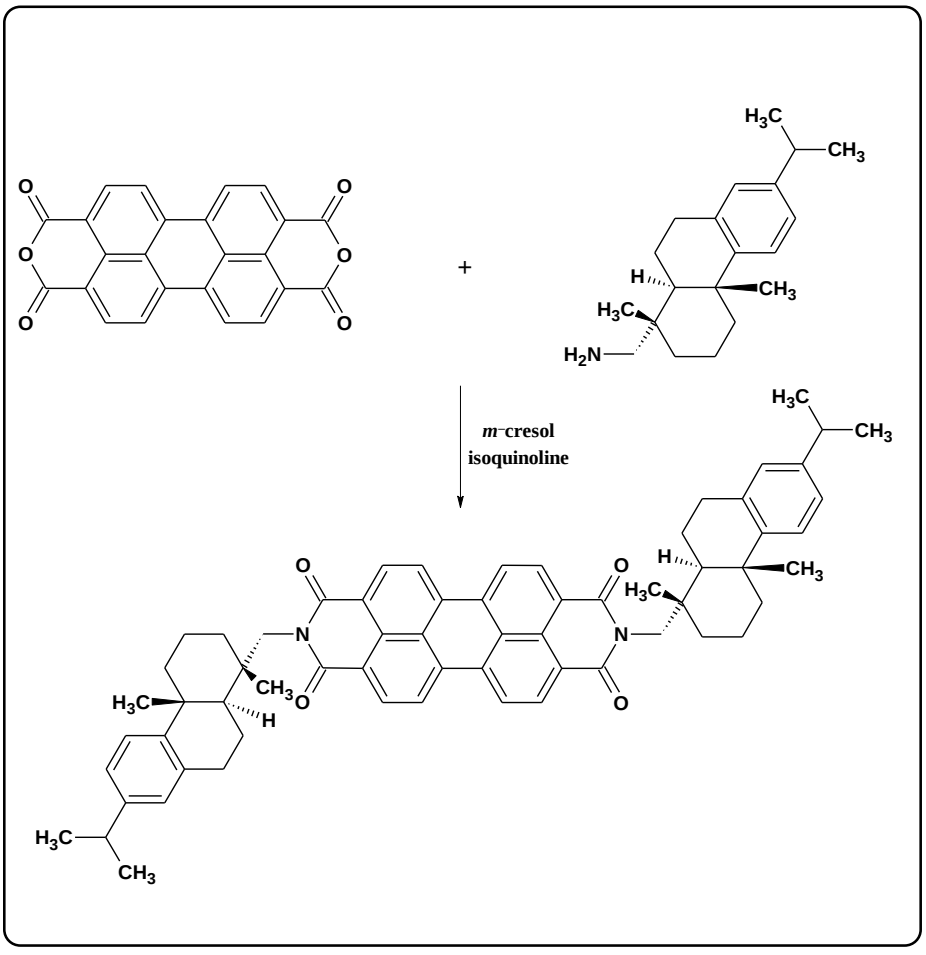

Scheme 3.1: Synthesis of N-N′-di (1-dehydroabietyl) perylene 3, 4, 9, 10-bis (Dicarboxymide) (ABPDI)

Novel ABPMI was synthesized from ABPDI using isopropanol, KOH and water according to the published procedure (Scheme 3.2) [37].

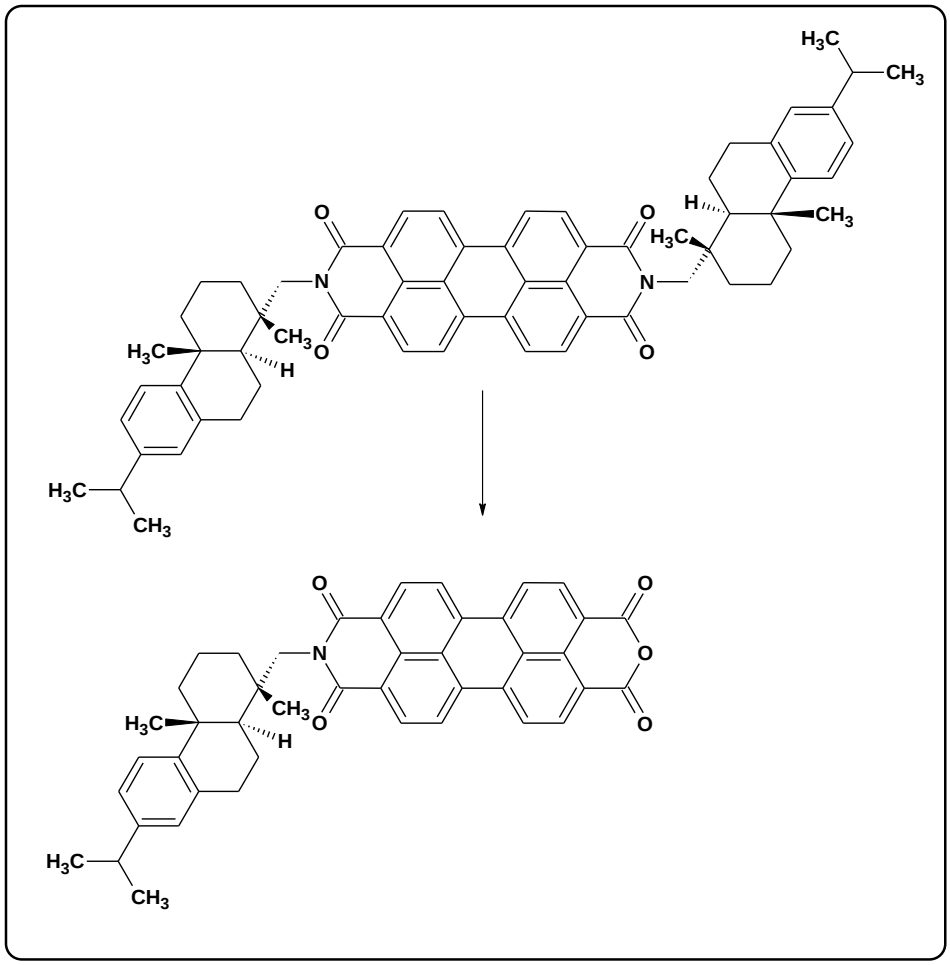

Scheme 3.2: Synthesis of N-(1-dehydroabietyl) - 3, 4, 9, 10-perylenetetracarboxylic-3, 4-anhydride-9, 10-imide (ABPMI)

3.3.1 Synthesis of N-N′-di (1-dehydroabietyl) perylene 3, 4, 9, 10-bis (Dicarboxymide) (ABPDI)

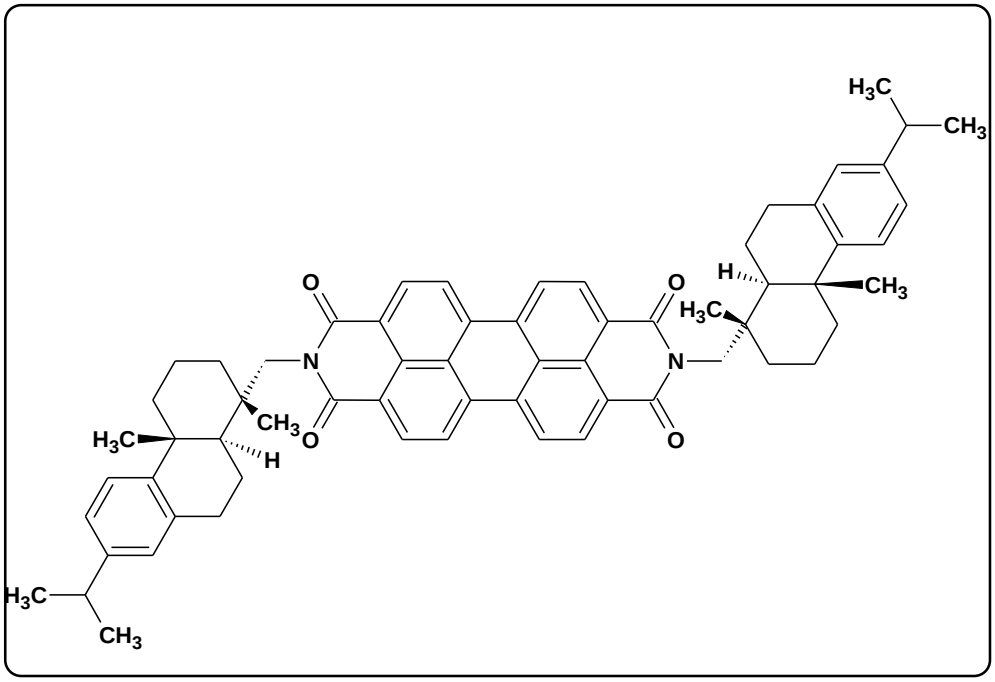

N-N′-di (1-dehydroabietyl) perylene 3, 4, 9, 10-bis (Dicarboxymide) (ABPDI) was synthesized successfully and characterized according to the published procedure [36].

3.3.2 Synthesis of N-(1-dehydroabietyl) - 3, 4, 9, 10-perylenetetracarboxylic-3, 4-anhydride-9, 10-imide (ABPMI)

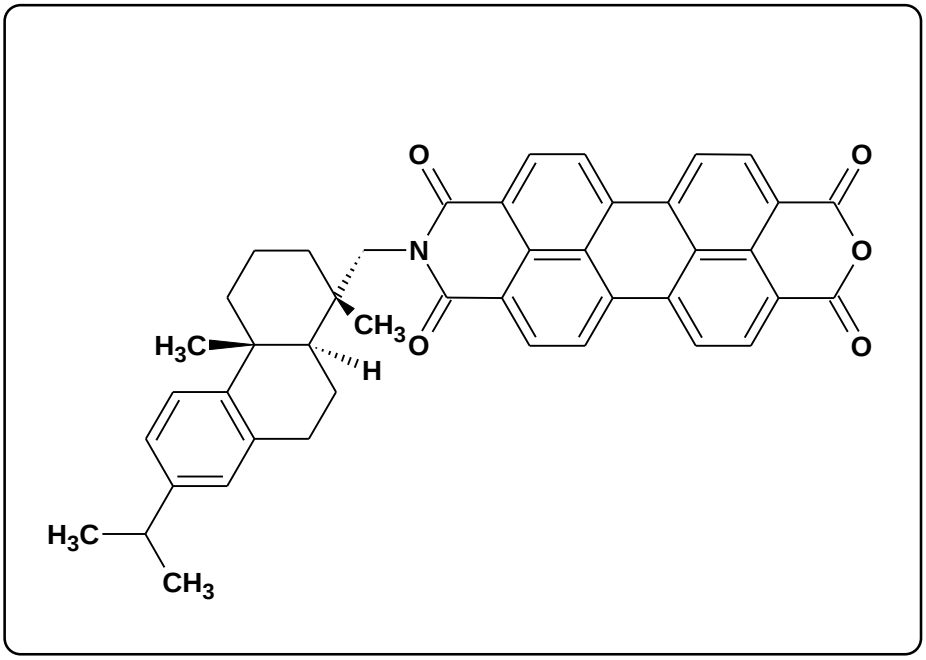

A suspension of synthesized N-N′-di (1-dehydroabietyl) perylene 3, 4, 9, 10-bis (Dicarboxymide) (ABPDI) (1.006 g, 1.085 mmol) and KOH (3.030 g, 54.01 mmol) in isopropyl alchohol (35.98 mL) and water (5.14 mL) was stirred for 20 min at room temperatre. Then, the reaction mixture was stirred under reflux at 82^0C for 55 h. In order to obtain precipates, the reaction mixture was poured into the dilute HCl (51.40 mL) to take precipitates. The precipitates were filtered off and washed with water. The product, first, purified by Soxhlet apparatus in methanol for 25 h. Further purification by recrystallization from chloroform (300 mL) was used to obtain a pure red solid monoimide, ABPMI. The pure product was dried in vacuum oven at 110^0 C.

Yield: 96.18 % (2.28 g), Color: red solid

FT-IR (KBr, cm^{-1}): υ = 3414, 2959, 2927, 2869, 1775, 1707, 1656, 1594, 1456, 1382, 1288, 1021, 820, 806.

UV-vis ($CHCl_3$)(λ_{max}/nm(ε_{max}/$L.mol^{-1}.cm^{-1}$)): 439 (125000), 469 (134000), 517 (135000)

Fluorescence ($CHCl_3$(λ_{max}/ nm): 536, 573

Q_f = 0.45

3.4 General Reaction Mechanisms of Perylene imide Derivatives

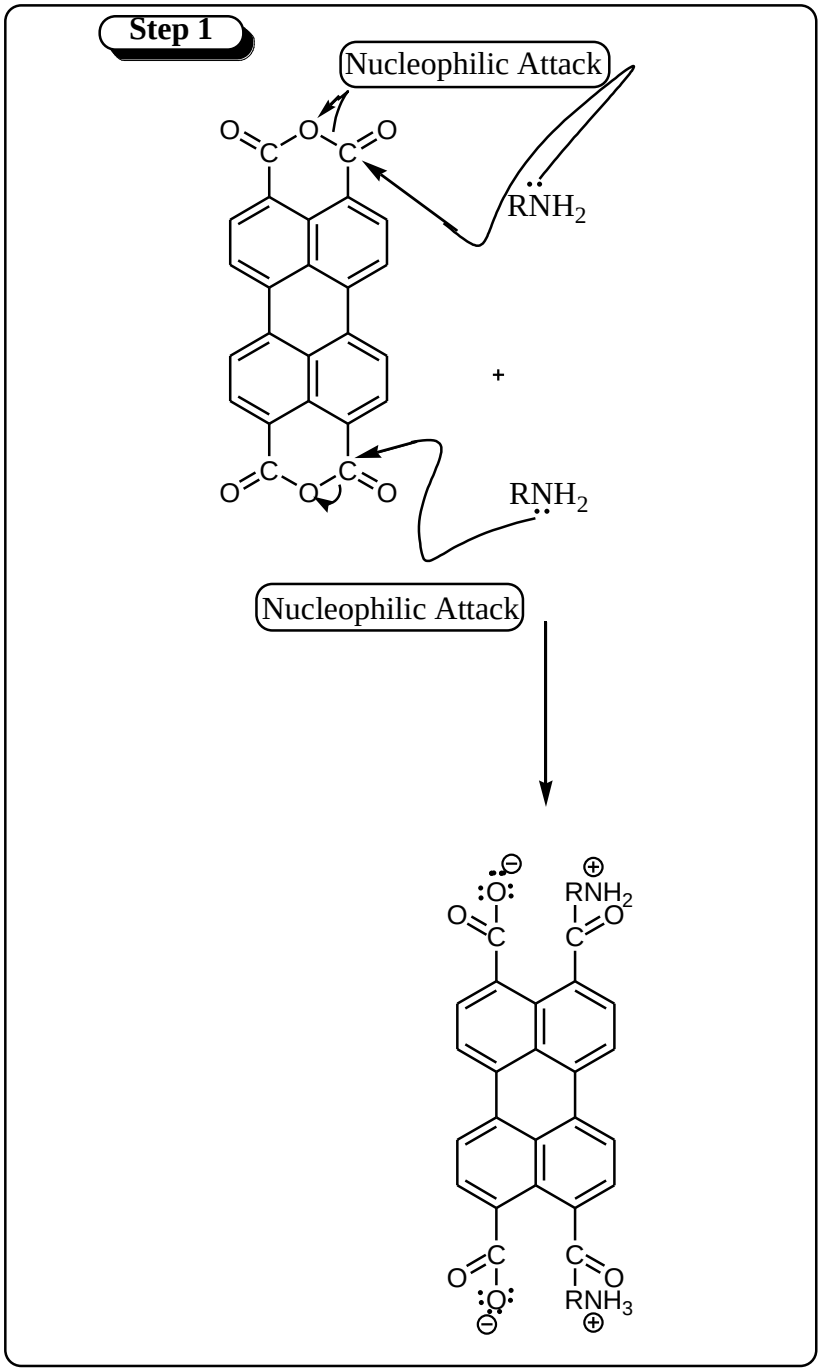

Step 2

Proton Abstraction

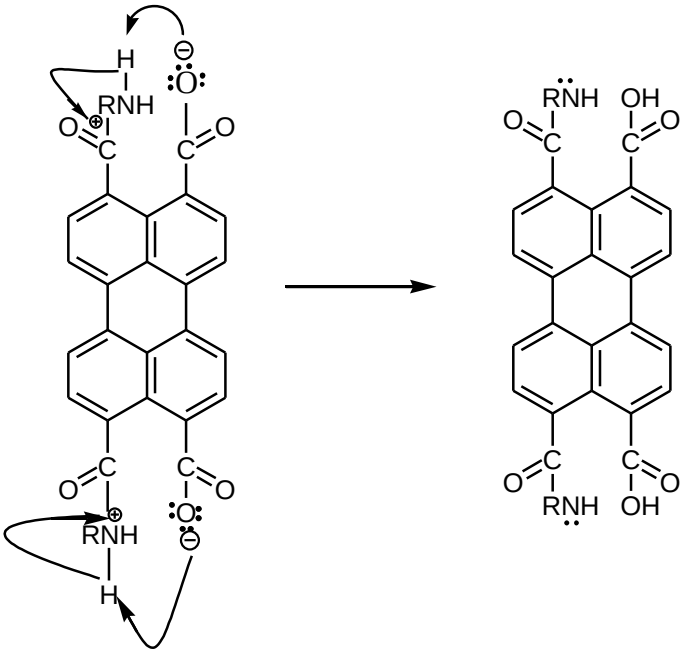

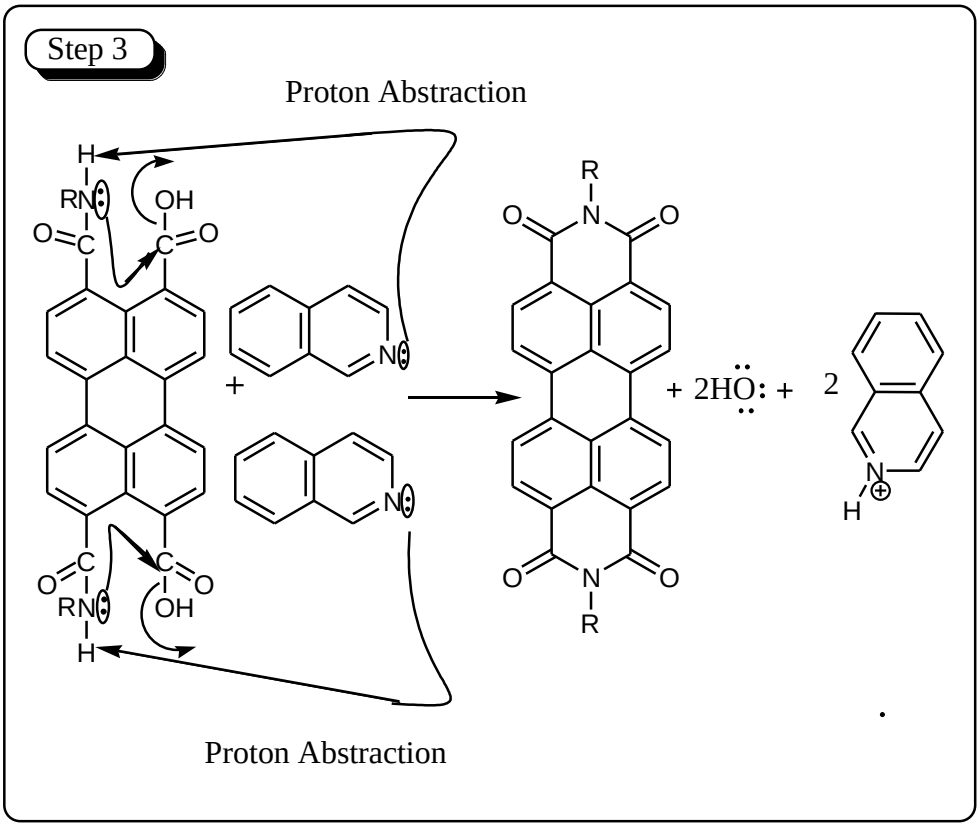
Step 3
Proton Abstraction
Proton Abstraction

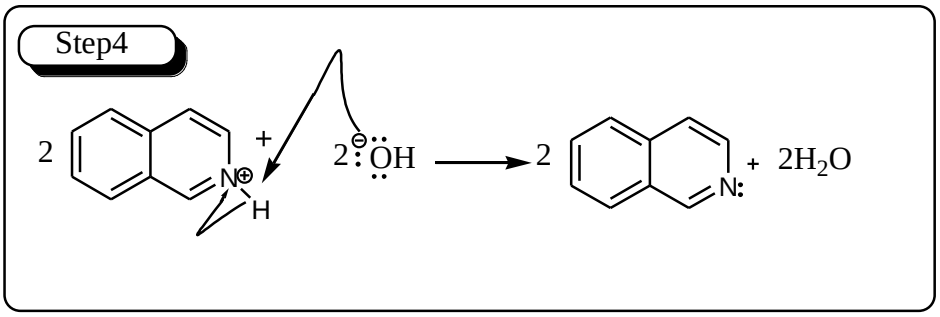
Step4

Chapter 4

DATA AND CALCULATION

4.1 Calculations of Fluorescence quantum yield, Φ_f

Fluorescence quantum yield, Q_f of the synthesized compounds calculated by using equation 4.1:

$$\Phi_f=\left(\frac{A_{std}}{A_u}\right)\left(\frac{S_u}{S_{std}}\right)\left(\frac{n_u}{n_{std}}\right)^2(\Phi_f) \quad (4.1)$$

Where:

Φ_f(U): Fluorescence quantum yield of unknown

A_{std}: Absorbance of reference at the excitation wavelength

A_u: Absorbance of unknown at the excitation wavelength

S_u: The integrated emission area across the band of unknown

S_{std}: The integrated emission area across the band of reference

n_u: Refractive index of unknown solvent

n_{std}: Refractive index of refrence solvent

The fluorescence quantum yields of perylene dyes were measured at the excitation wavelength of 485 nm (λ_{max}= 485 nm) together with refrence. The N,N′-bis(dodecyl)-3,4,9,10-perylenebis(discarboximide) was used as refrence in the calculations (Φ_f = 1 in chloroform) [37].

Φ_f calculation of ABPDI in CHL:

The reference is N,N′-bis (dodecyl)-3,4,9,10-perylenebis (discarboximide)

A_{std} = 0.1055

A_u = 0.1078

S_u = 4209.78

S_{std} = 4129.22

n_u = 1.446

n_{std} =1.446

Φ_{std} =1.0

$$\boldsymbol{\Phi_f = \frac{0.1055}{0.1078} \times \frac{4209.78}{4129.22} \times \left[\frac{1.446}{1.446}\right]^2 \times 1 = 1}$$

$\Phi_{f,ABPDI}$ =1

The Table 4.1 shows the calculated fluorescence quantum yield (Φ_f) values of ABPDI and ABPMI in CHL.

Table 4.1: The fluorescence quantum yield of ABPDI and ABPMI in CHL

Compound	$\mathbf{Q_f}$
ABPDI	1
ABPMI	0.45

4.2 Calculations of Molar absorptivity, ε_{max}

At a given wavelength, the molar absorptivity measures how strongly a chemical substance absorbs light. The Beer-Lambert Law (Eq 4.2) is used for calculation of ε_{max} of the synthesized ABPDI and ABPMI [38].

$$\boldsymbol{\varepsilon_{max} = \frac{A}{c.l}} \quad (4.2)$$

Where:

ε_{max}: Molar absorption coefficient ($L.mol^{-1}.cm^{-1}$)

A: Absorbance

c: Concentration ($mol.L^{-1}$)

l: Cell length (1cm)

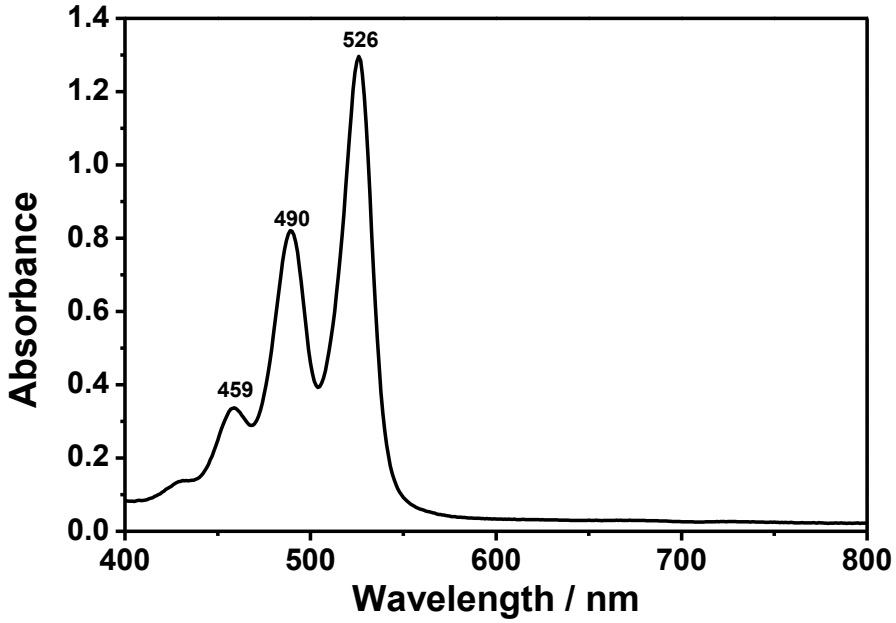

Figure 4.1: Absorption Spectrum of ABPDI in CHL at ($c=1\times10^{-5}$ M)

ε_{max} calculation in CHL:

c = 1.00×10^{-5} M in chloroform;

l = 1cm

At λ = 526nm, A= 1.3

$\varepsilon_{max} = \frac{1.3}{1\times10^{-5}M\times1cm}$ = 130000 $L.mol^{-1}.cm^{-1}$

The ε_{max} values of the synthesized compounds in different solvents were calculated using equation 4.2 (Table 4.1).

Table 4.2: Molar extinction coefficient data of ABPID and ABPMI in different solvents

Compound	Solvent	λ_{max}	ε_{max} (L.mol^{-1}.cm^{-1})
ABPDI	CHL	525	130000
	DMF	526	115000
	MeOH	521	56000
ABPMI	CHL	517	135000
	DMF	518	113700
	MeOH	511	113000

4.3 Calculations of Half-Width of Selected Absorption , $\Delta\bar{\nu}_{1/2}$

The Half-Width of Selected Absorption was calculated from the equation 4.3 with the absorption spectra of the ABPDI and ABPMI [38].

$$\Delta\bar{\nu}_{1/2} = \bar{\nu}_{I} - \bar{\nu}_{II} \quad (4.3)$$

Where

$\bar{\nu}_{I}$ and $\bar{\nu}_{II}$: The frequencies from the absorption spectra in cm^{-1}

$\Delta\bar{\nu}_{1/2}$: Half-width of Selected Absorption in cm^{-1}

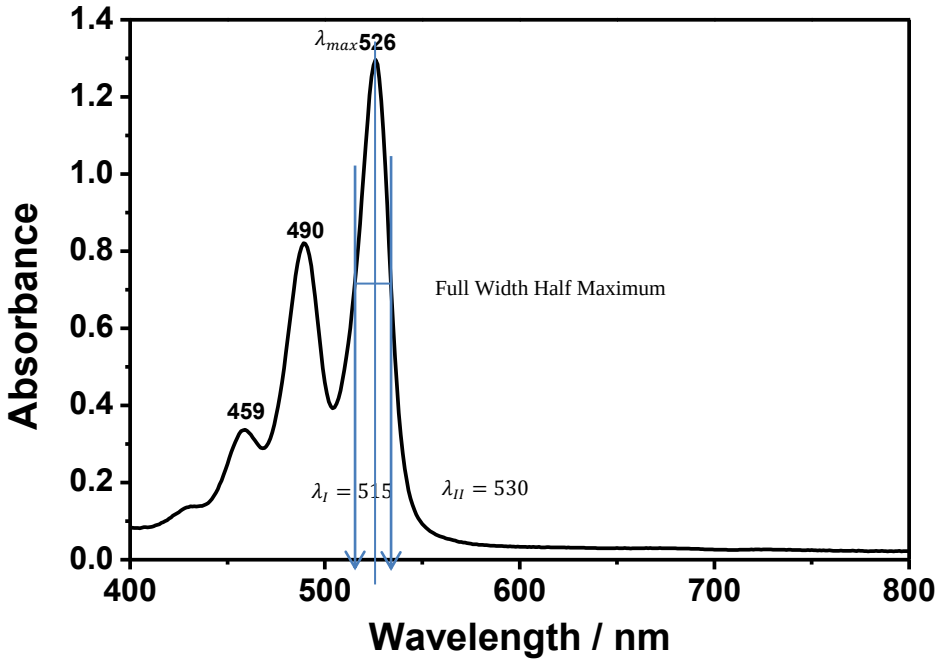

Figure 4.2: Absorption spectrum for ABPDI in CHLand related half-width of ε_{max}

When λ_I = 515nm, in CHL for ABPDI:

⇨ $\lambda_I = 5.15\text{nm} \times \frac{10^{-9}m}{1nm} \times \frac{10^{2}cm}{1m} = 5.15 \times 10^{-5}$ cm

⇨ $\bar{\nu}_I = \frac{1}{5.15\times10^{-5}cm} = 19417.4757\ \text{cm}^{-1}$

When λ_{II} =530 nm:

⇨ $\lambda_{II} = 530\text{nm} \times \frac{10^{-9}m}{1nm} \times \frac{10^{2}cm}{1m} = 5.3\times 10^{-5}$ cm

⇨ $\bar{\nu}_{II} = \frac{1}{5.3\times10^{-5}cm} = 18867.9245\ \text{cm}^{-1}$

⇨ $\Delta\bar{\nu}_{1/2} = \bar{\nu}_{\text{initial}} - \bar{\nu}_{\text{final}}$

⇨ $19417.4757 - 18867.9245 = 549.5511\ \text{cm}^{-1}$

$\Delta\bar{\nu}_{1/2} = 549.5511\ \text{cm}^{-1}$

When λ_I= 518 nm, in CHL for ABPMI:

$\lambda_I = 4.90\text{ nm} \times (\frac{10^{-9}m}{1nm}) \times (\frac{10^{2}cm}{1m}) = 4.90 \times 10^{-5}$ cm

$\bar{\nu}_I = \frac{1}{4.90\times10^{-5}cm} = 20408.1632\text{cm}^{-1}$

$\lambda_{II} = 575\text{ nm} \times (\frac{10^{-9}m}{1nm}) \times \left(\frac{10^{2}cm}{1m}\right) = 5.75 \times 10^{-5}$ cm

$\bar{\nu}_{II} = \frac{1}{5.75\times10^{-5}cm}$ = 17391.3043 cm^{-1}

$\Delta\bar{\nu}_{1/2} = \bar{\nu}_{initial} - \bar{\nu}_{final}$

20408.1632─ 17391.3043 = 3016.8589cm^{-1}

$\Delta\bar{\nu}_{1/2}$ = 3016.8589 cm^{-1}

The $\Delta\bar{\nu}_{1/2}$ values of ABPDI and ABPMI were calculated in different solvents and the data was tabulated in Table 4.3.

Table 4.3: Half-Width of Selected Absorption for ABPDI and ABPMI in different solvents

Compound	**Solvent**	**λ_I(cm)**	**λ_{II}(cm)**	**$\Delta\nu_{1/2}$ (cm^{-1})**
ABPDI	CHL	5.15×10^{-5}	5.30×10^{-5}	549.50
	DMF	5.10×10^{-5}	5.40×10^{-5}	1089.30
	MeOH	5.00×10^{-5}	5.60×10^{-5}	2142.80
ABPMI	CHL	4.90×10^{-5}	5.75×10^{-5}	3016.80
	DMF	5.00×10^{-5}	5.20×10^{-5}	769.230
	MeOH	4.80×10^{-5}	5.70×10^{-5}	3289.50

4.4 Calculations of Theoretical Radiative Lifetime, τ_0

Equation 4.4 was used to calculate the theoretical radiative lifetime (τ_0)

$$\boldsymbol{\tau_0 = \frac{3.5\times10^{8}}{\upsilon_{max}^{2}\times\varepsilon_{max}\times\Delta\bar{\upsilon}_{1/2}}} \quad (4.4)$$

Where:

τ_0 : Theoretical radiative lifetime in ns

ν_{max}: Mean frequency of the maximumabsorption band in cm^{-1}

ε_{max}: The maximum molar absorptivity at maximum absorption wavelength in $L.mol^{-1}.cm^{-1}$

$\Delta\bar{\nu}_{1/2}$: Half-width of the selected absorption in unit of cm^{-1}

Calculation of τ_0 for ABPDI in CHL:

At λ_{max} = 526nm , ε_{max}= 130000 $L.mol^{-1}.cm^{-1}$

λ_{max}=526nm×$\frac{10^{-9}m}{1nm}$×$\frac{10^{2}cm}{1m}$= $5.26\times10^{-5}cm^{-1}$

ν_{max}= $\frac{1}{\lambda_{max}}$ = $\frac{1}{5.26\times10^{-5}cm}$ = 19011.4068 cm^{-1}

ν^2_{max}= (19011.4068 cm^{-1})^2 = 3.60×10^{8} cm^{-2}

$\Delta\bar{\nu}_{1/2}$ = 549.50 cm^{-1}

τ_0= $\frac{3.5\times10^{8}}{3.6\times10^{8}cm^{-2}\times130000L.mol^{-1}.cm^{-1}\times549.50\ cm^{-1}}$ = 0.001360×10^{-5} sec

τ_0= 0.001360×10^{-5} sec×$\frac{1ns}{10^{-9}sec}$ = 13.6 ns

Table 4.4: Theoretical radiative lifetime for ABPDI and ABPMI in different solvents

Compound	**Solvent**	**λ_{max} (nm)**	**ε_{max} ($L.mol^{-1}.cm^{-1}$)**	**ν^2_{max} (cm^{-2})**	**$\Delta\bar{\nu}_{1/2}$ (cm^{-1})**	**η_0 (ns)**
ABPDI	CHL	526	130000	3.60×10^{8}	549.50	13.60
	DMF	525	115000	3.60×10^{8}	1089.30	7.80
	MeOH	521	56000	3.60×10^{8}	2142.80	8.40
ABPMID	CHL	517	135000	3.70×10^{8}	3016.80	2.30
	DMF	518	113700	3.70×10^{8}	769.23	10.80
	MeOH	511	113000	3.80×10^{8}	3289.50	2.50

4.5 Calculations of Theoretical Fluorescence Lifetime, τ_0

The fluorescence lifetime shows the average time that molecule stays at the excited state. The data were calculated according to the following equation.

$$\tau_f = \tau_0 . \Phi_f \quad (4.5)$$

Where:

τ_0 : Theoretical radiative lifetime in ns

τ_f : Theoretical fluorescent lifetime in ns

Φ_f : Fluorescence quantum yield

Calculation of τ_f for ABPDI in CHL:

$\tau_f = 13.60 \times 1 = 13.60$ ns

Calculation of τ_f for ABPMI in CHL:

$\tau_f = 2.30 \times 0.45 = 1.035$ ns

Theoretical fluorescence lifetime (τ_f) data calculated in CHL were tabulated in Table 4.5.

Table 4.5: Theoretical fluorescence lifetime for ABPDI and ABPMI in CHL

Compound	**τ_f(ns)**
ABPDI	13.60
ABPMI	1.035

4.6 Calculations of Theoretical Fluorescence Rate Constant, kf

The formula illustrated below is used to calculate the theoretical fluorescence rate constant for synthesized perylene derivatives [39]:

$$k_f = \frac{1}{\tau_0} \quad (4.6)$$

Where:

k_f : Fluorescent rate constant in s^{-1}

τ_0 : Theoretical radiative lifetime in s

Calculation of k_f for ABPDI in CHl:

$k_f = \frac{1}{13.60} = 0.0735\ s^{-1}$

Table 4.6: Theoretical fluorescence rate constant of ABPDI in different solvents

Compound	Solvent	$k_f(s^{-1})$
ABPDI	CHL	0.0735
	DMF	0.1282
	MeOH	0.1190
ABPMI	CHL	0.4347
	DMF	0.0925
	MeOH	0.4000

4.7 Calculations of Oscillator Strength, f

The dimensionless value oscillatorstrenght was calculated according to equation 4.7

$$f = 4.32 \times 10^{-9} \times \Delta\bar{\nu}_{1/2} \times \varepsilon_{max} \quad (4.7)$$

Where:

f: Oscillator strength in $mol^{-1}.cm^{-2}$

$\Delta\bar{\nu}_{1/2}$: Half-width of selected absorption in cm^{-1}

ε_{max}: Maximum absorption coefficient in $L.mol^{-1}.cm^{-1}$ at λ_{max}

Calculation of Oscillator Strength for ABPDI in CHl:

$f = 4.32\times10^{-9}\times549.50\ cm^{-1}\times130000 L.mol^{-1}.cm^{-1} = 0.3085\ L.mol^{-1}.cm^{-2}$

$f = L.mol^{-1}.cm^{-2}$

The calculated oscillator strength in different solvents was shown in Table 4.7.

Table 4.7: Calculations of oscillator strength for ABPDI in different solvents

Compound	**Solvent**	***f* ($mol^{-1}.cm^{-2}$)**
ABPDI	CHL	0.3085
	DMF	0.5411
	MeOH	0.49987
ABPMI	CHL	1.7593
	DMF	0.3778
	MeOH	1.6058

4.8 Calculatios of Singlet Energy, E_s

Singlet energy of the synthesized compounds were calculated using the equation given below:

$$E_s = \frac{2.86\times10^5}{\lambda_{max}} \quad (4.8)$$

Where:

E_s = Singlet energy in $kcal.mol^{-1}$

λ_{max} = The maximum absorption wavelength in A^0

Calculation of singlet energy for ABPDI in CHL:

$E_s = \frac{2.86 \times 10^5}{5260}$ = 54.372 kcal.mol^{-1}

Similarly, the singlet energy of ABPDIand ABPMI were calculated in different solvents and the data shown in Table 4.8.

Table 4.8: Calculations of singlet energy data ABPDI and ABPMI in different solvents

Compound	**Solvent**	***Es*(kcal.mol^{-1})**
ABPDI	CHL	54.476
	DMF	54.372
	MeOH	54.894
ABPMI	CHL	55.319
	DMF	55.212
	MeOH	55.969

4.9 Calculations of Optical Band Gap Energy, E_g

The optical band gap energy of both ABPDI and ABPMI were calcualted uing the equation given below. The cut off absorption bands were obtained by extrapolating the maximum absorption bands to zero absorbance as shown in Figure 4.9.

$$\boldsymbol{E_g = \frac{1240 eV\ nm}{\lambda\ nm}} \quad (4.9)$$

Where:

E_g = Band gap energy in eV

λ = Cut off wavelength of the absorption band in nm

Calculations of Band Gap energy for ABPDI:

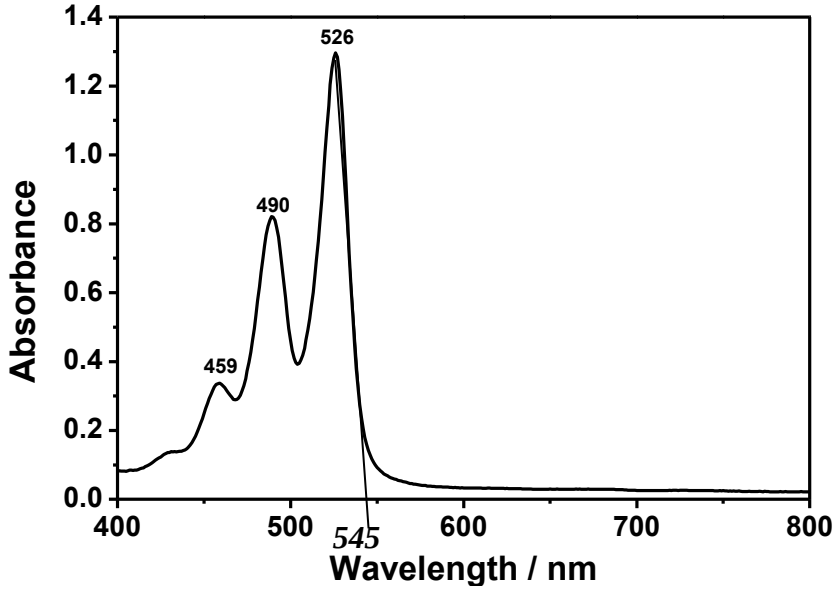

Figure 4.3: Representative figure for cut off absorption determinations

$E_g = \frac{1240\ e\ v}{545} = 2.275\ eV$

The results of E_g for ABPDI and ABPMI is shown in the following Table 4.9.

Table 4.9: Calculations of optical bandgap Energy of ABPDI and ABPMI in CHL

Compound	E_g**(eV)**
ABPDI	2.275
ABPMI	1.984

4.10 Thin Layer Chromatography (TLC) of ABPDI and ABPMI

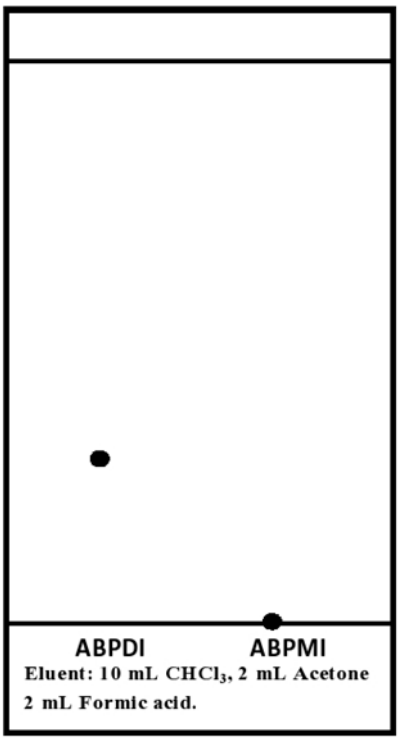

Figure 4.4: Thin layer chromatography of ABPDI and ABPMI (TLC)

The R_f value of ABPDI is equal to 25.0%. ABPMI is more polar than ABPDI as shown in the Figure 4.4.

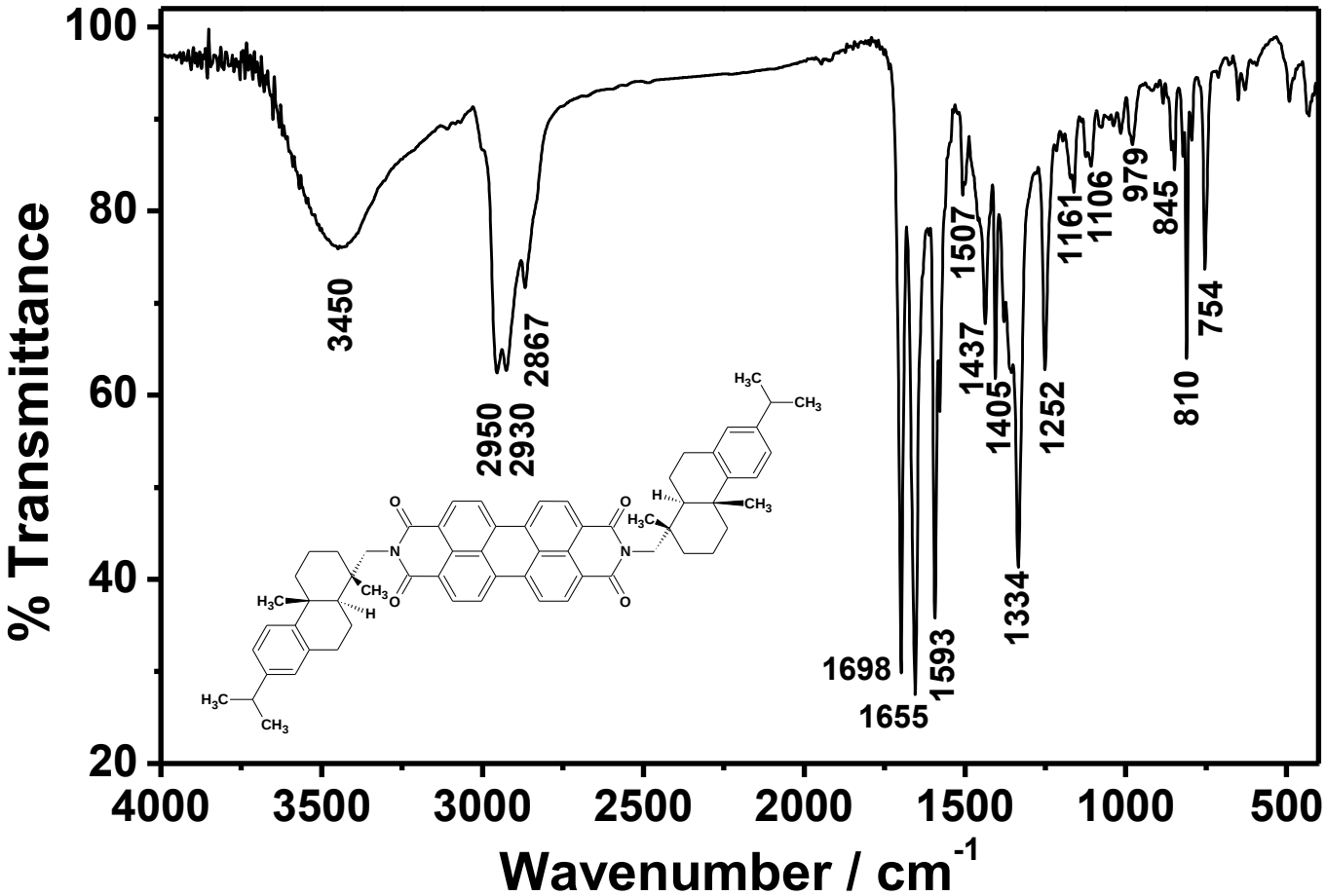

Figure 4.5: FTIR Spectrum of ABPDI

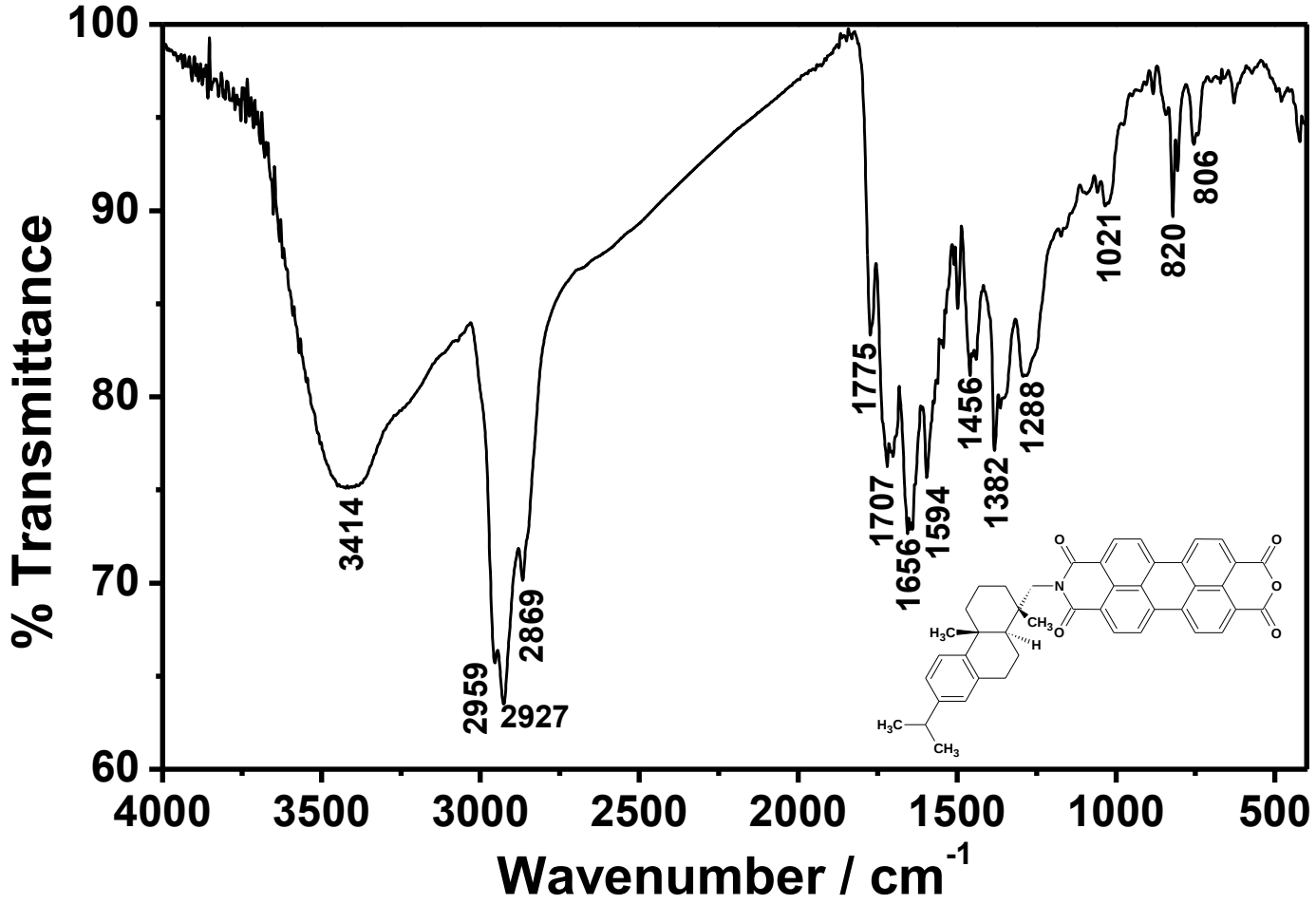

Figure 4.6: FTIR Spectrum of ABPMl

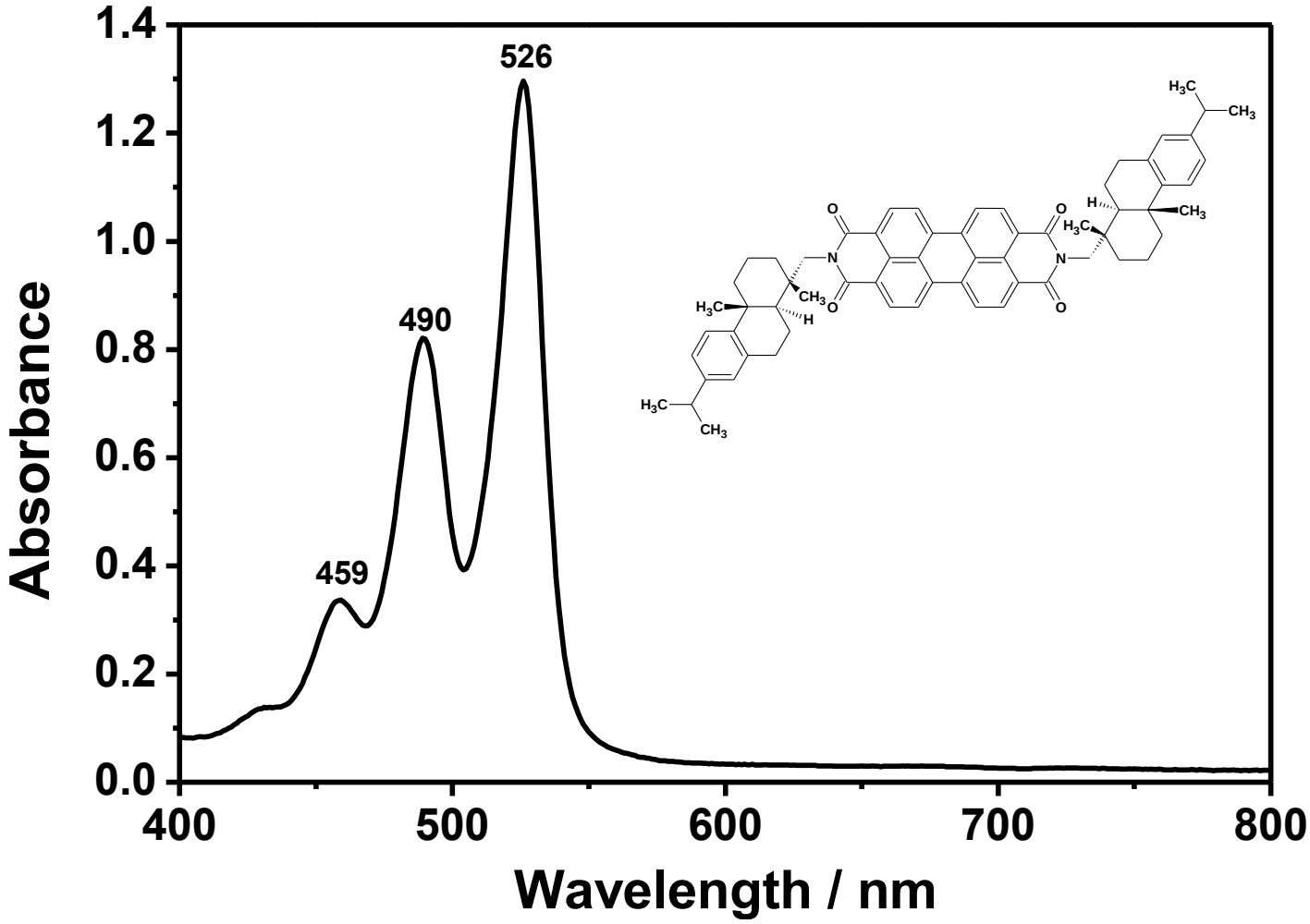

Figure 4.7: UV-Visible Absorption Spectrum of ABPDI in CHL

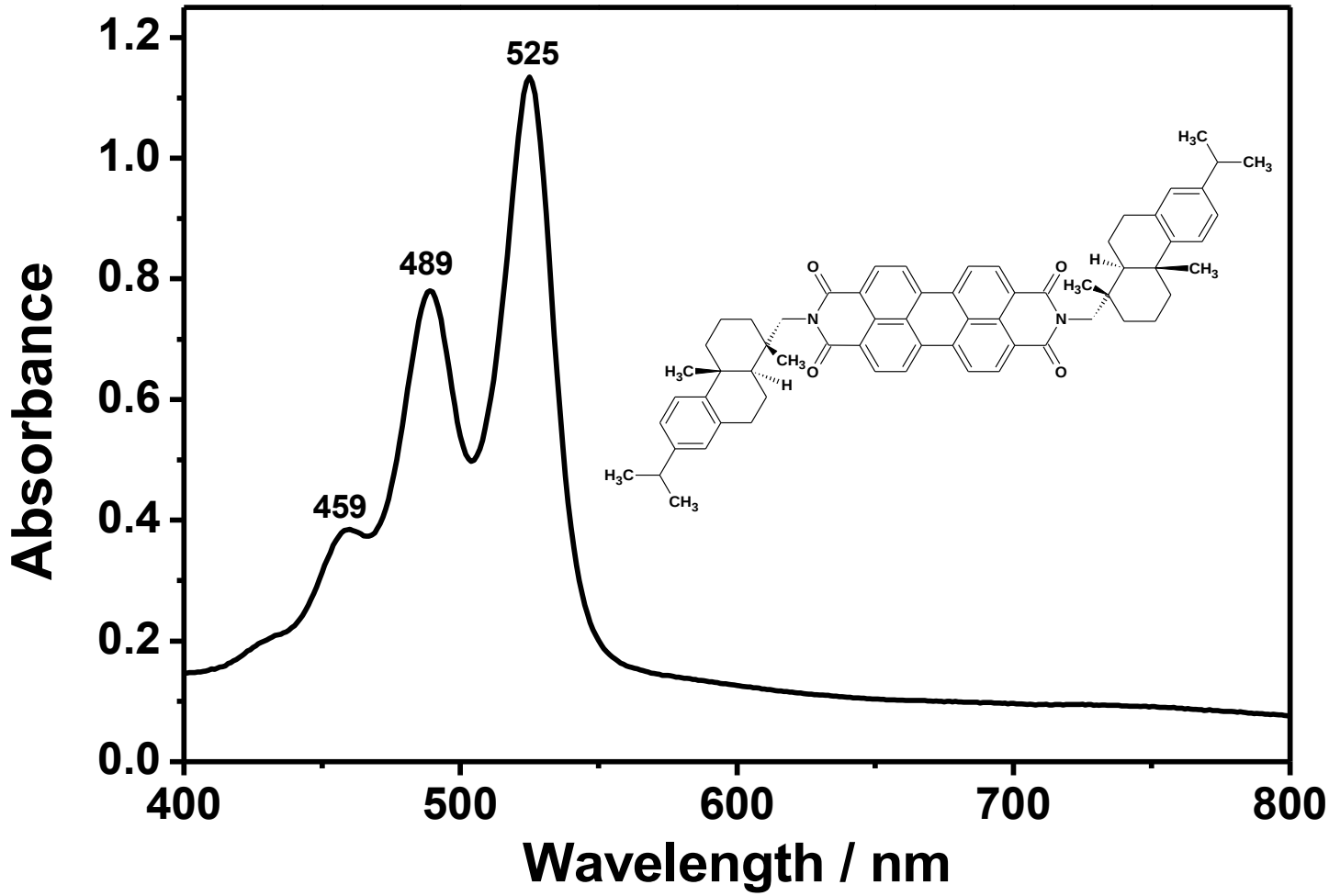

Figure 4.8: UV-Visible Absorption Spectrum of ABPDI in DMF

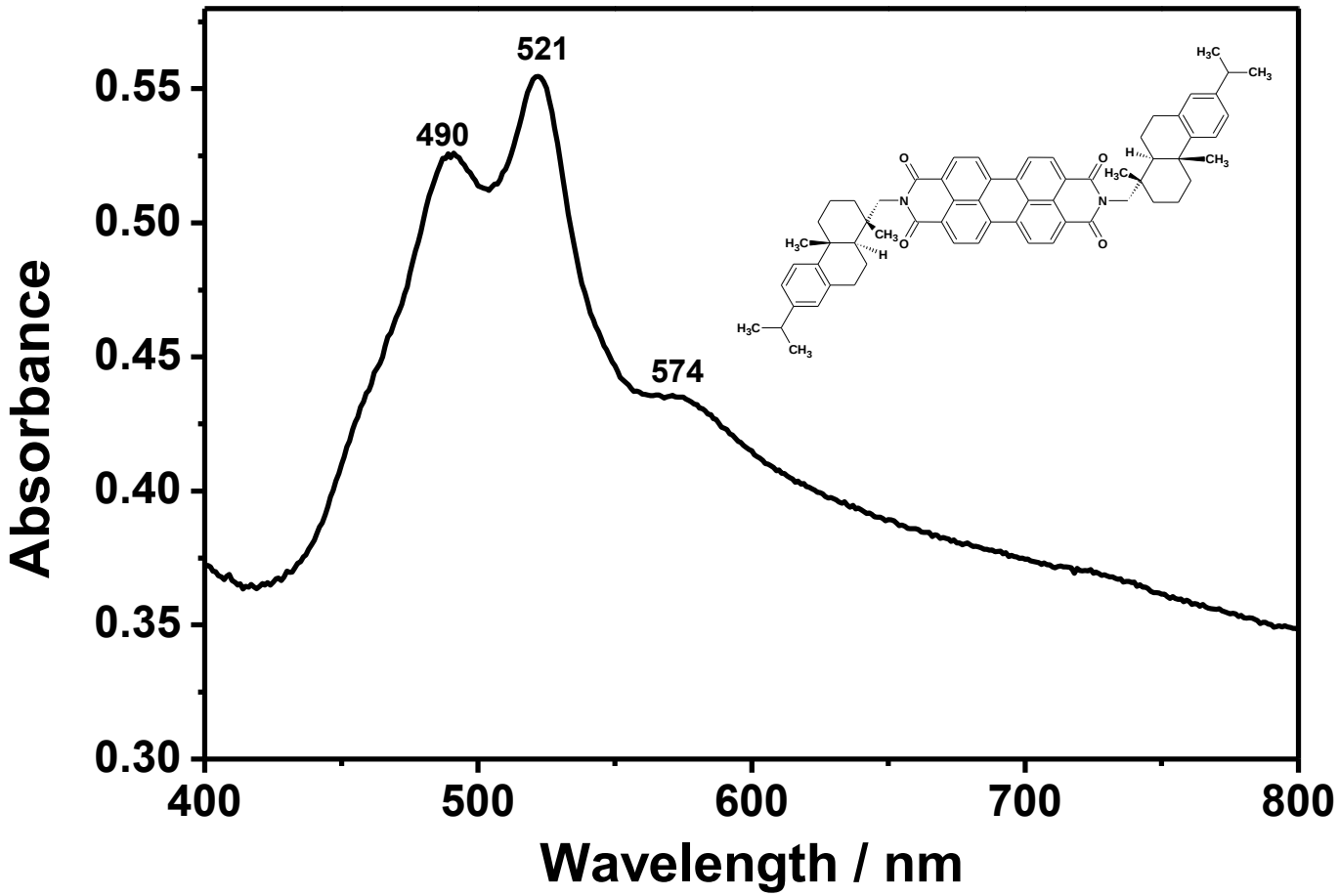

Figure 4.9: UV-Visible absorption spectrum of ABPDI in MeOH

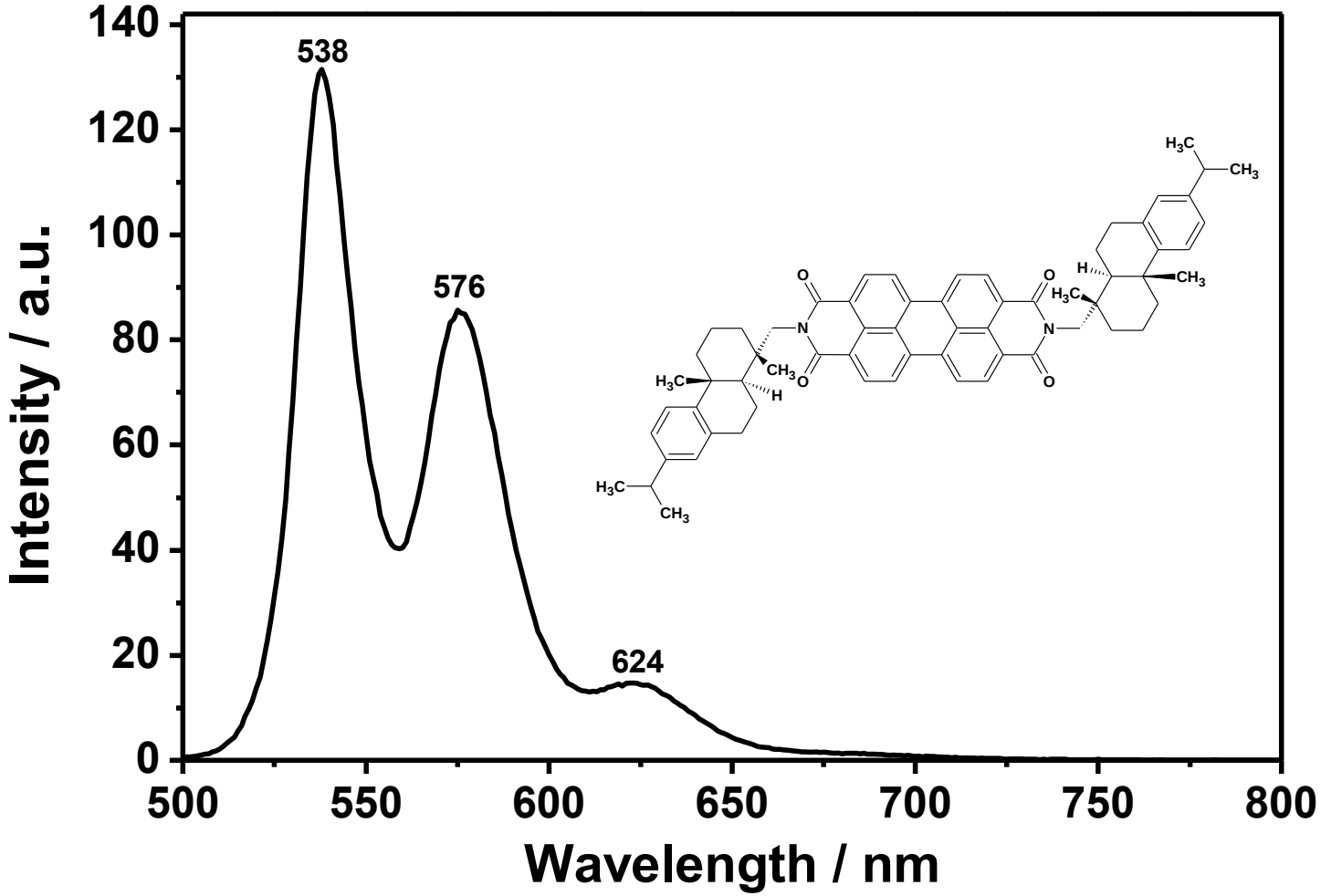

Figure 4.10: Emission Spectrum of ABPDI in CHL

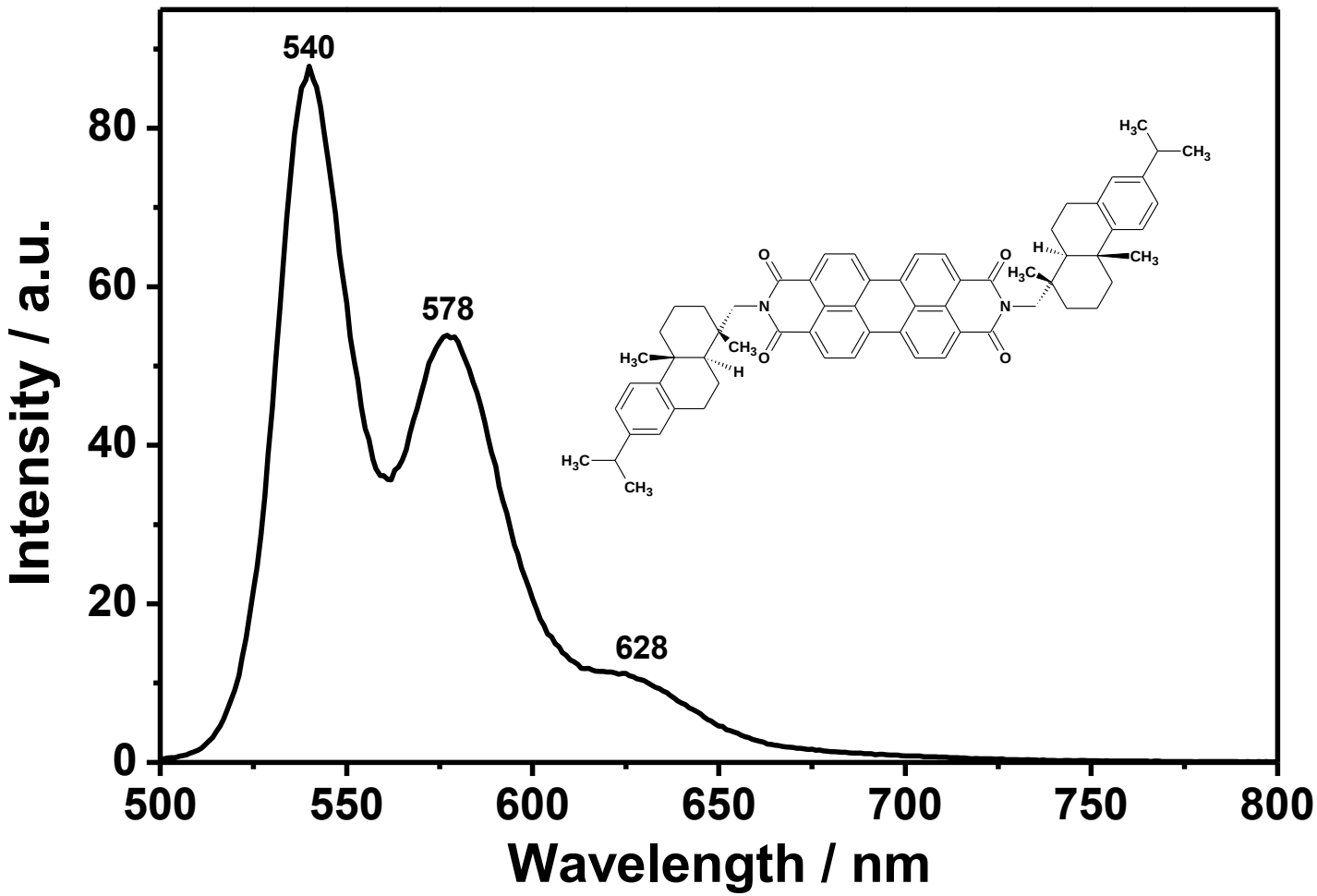

Figure 4.11: Emission Spectrum of ABPDI in DMF

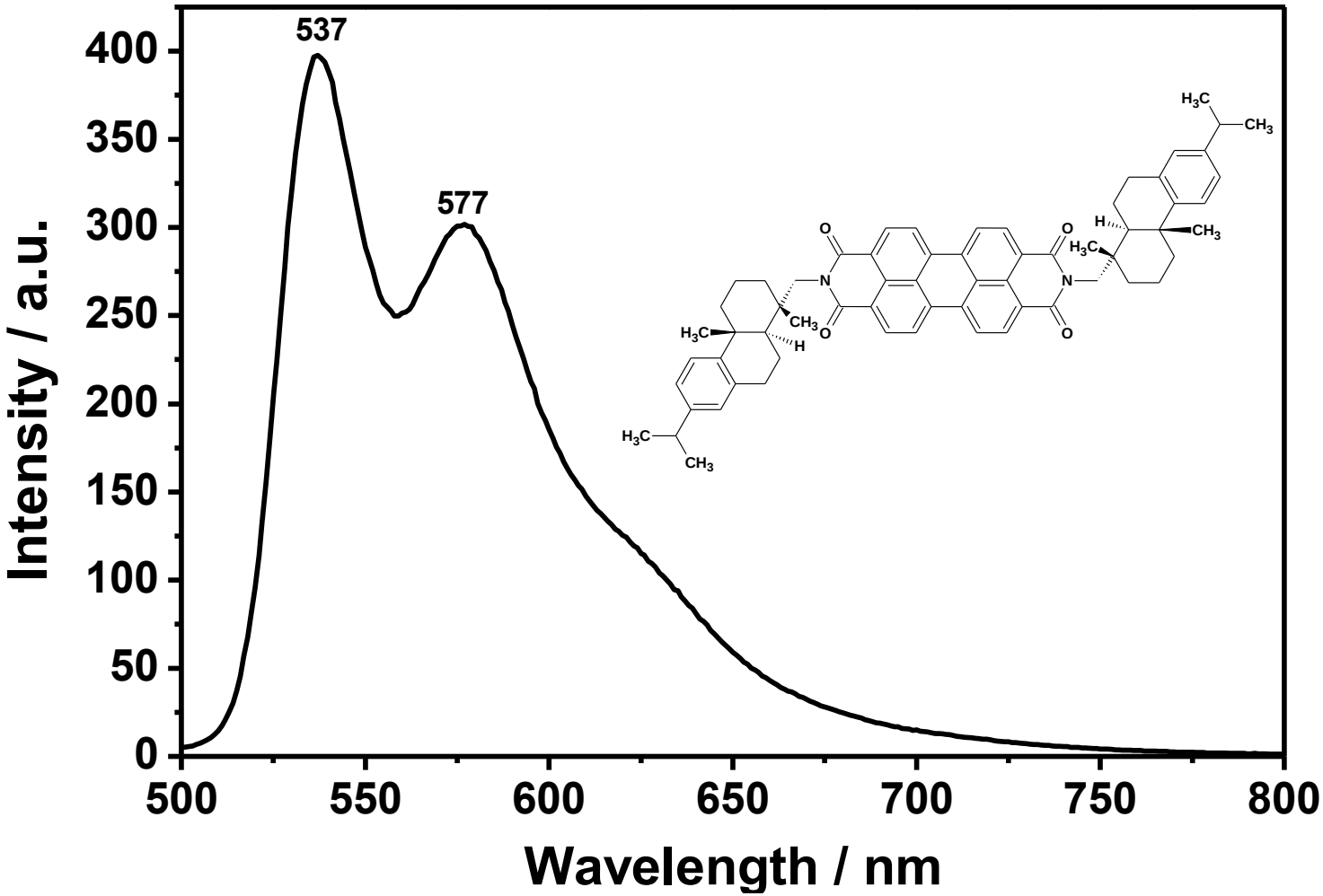

Figure 4.12: Emission Spectrum of ABPDI in MeOH

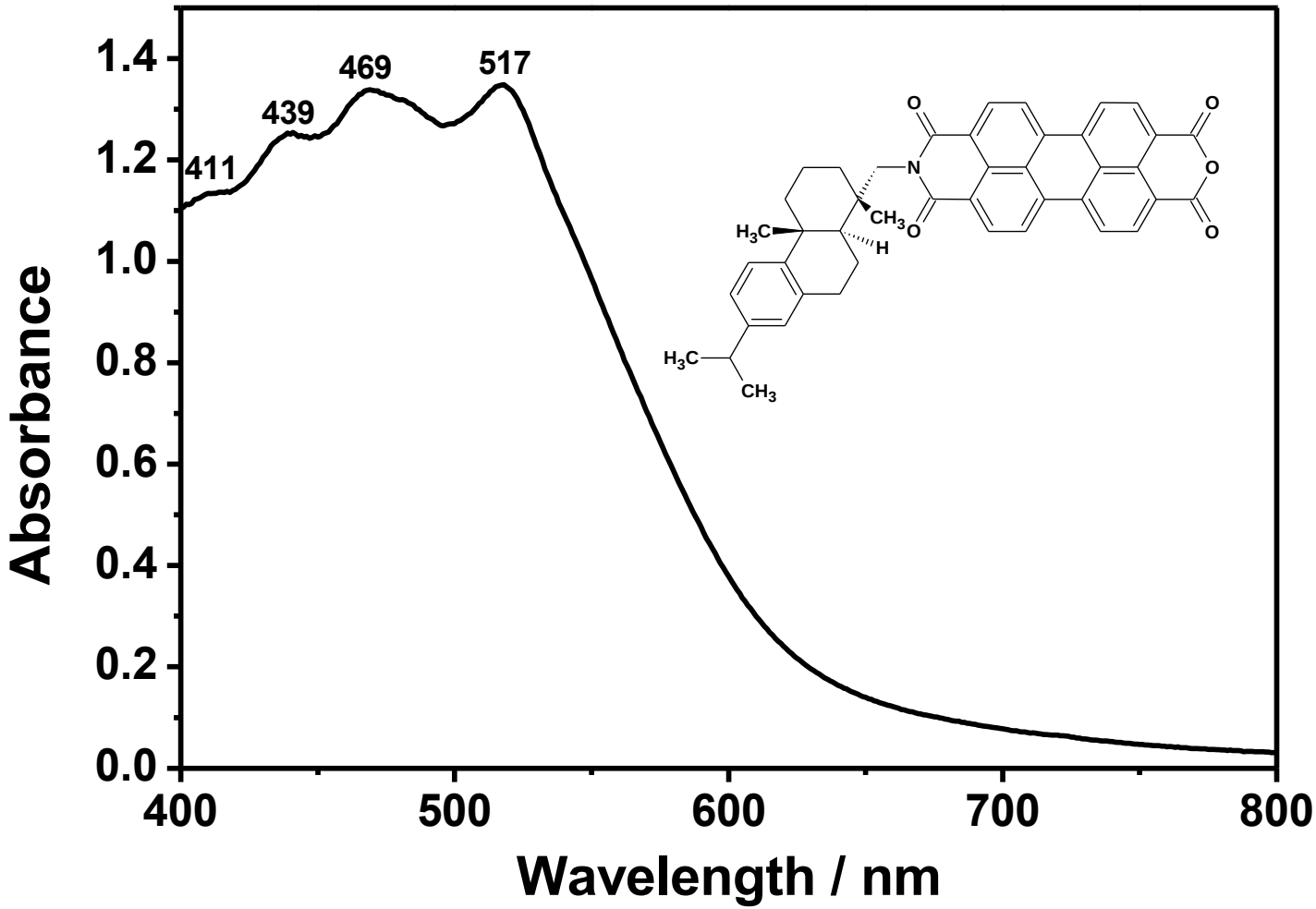

Figure 4.13: UV-Visible Absorption Spectrum of ABPMI in CHL

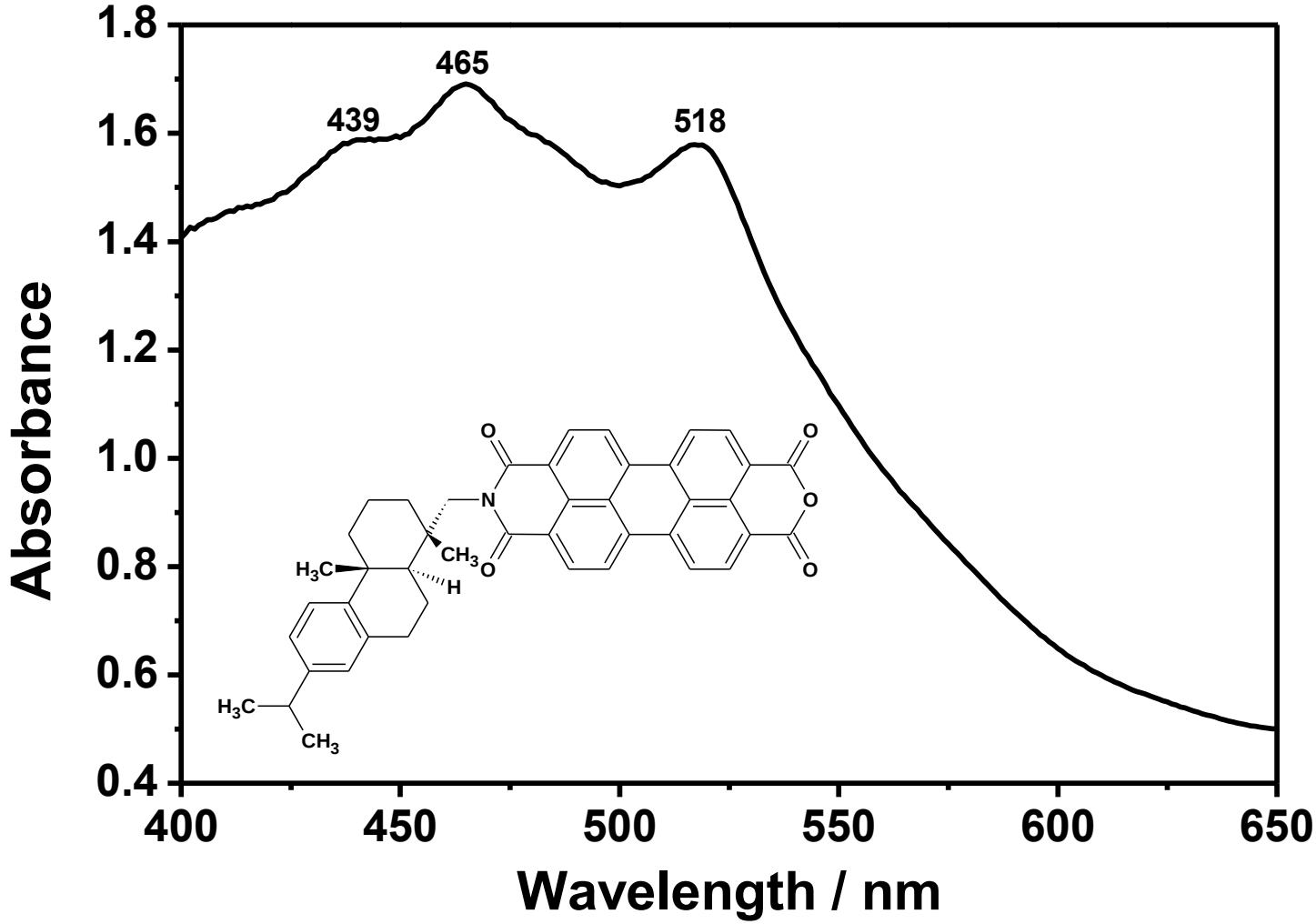

Figure 4.14: UV-Visible Absorption Spectrum of ABPMI in DMF

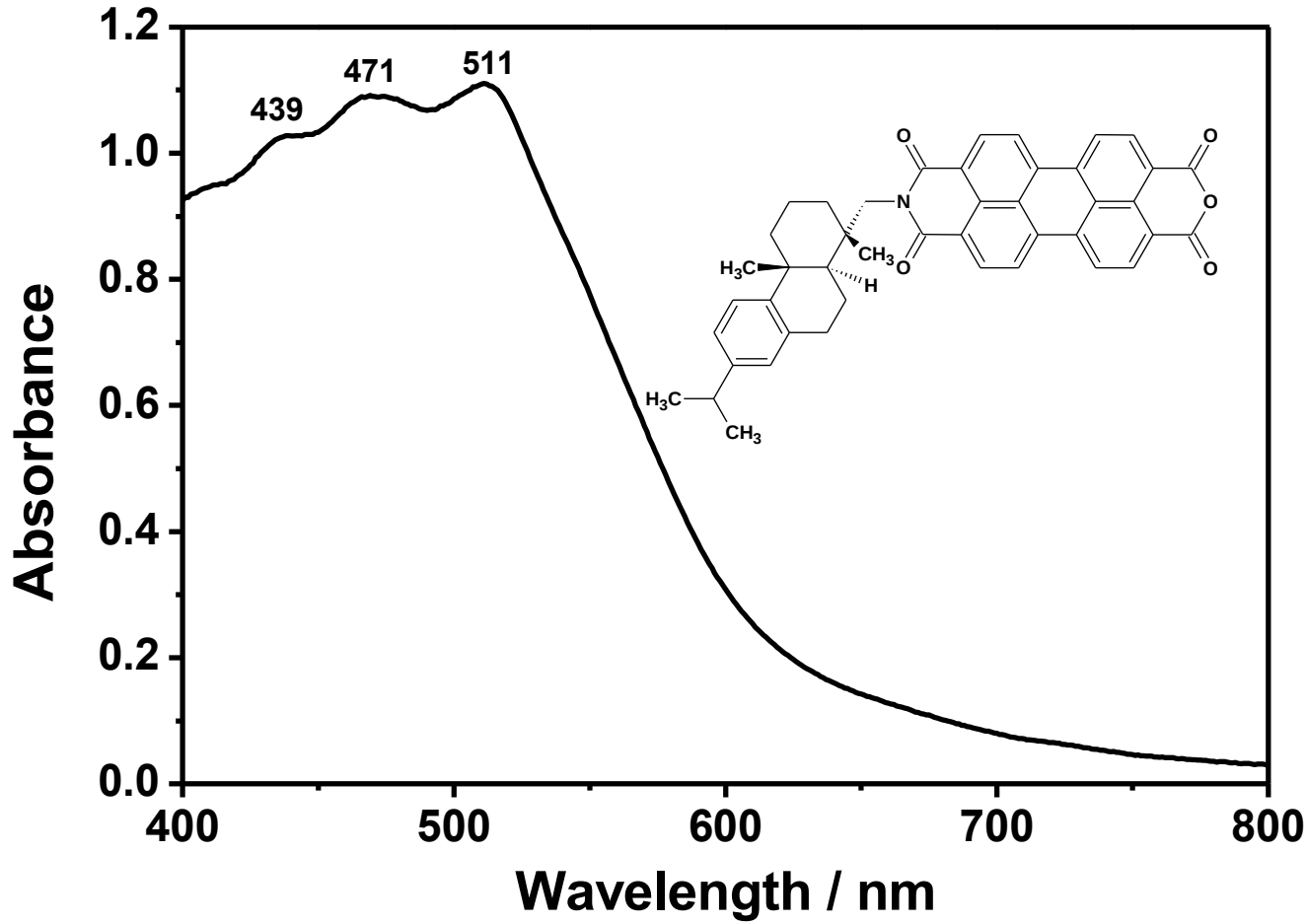

Figure 4.15: UV-Visible Absorption Spectrum of ABPMI in MeOH

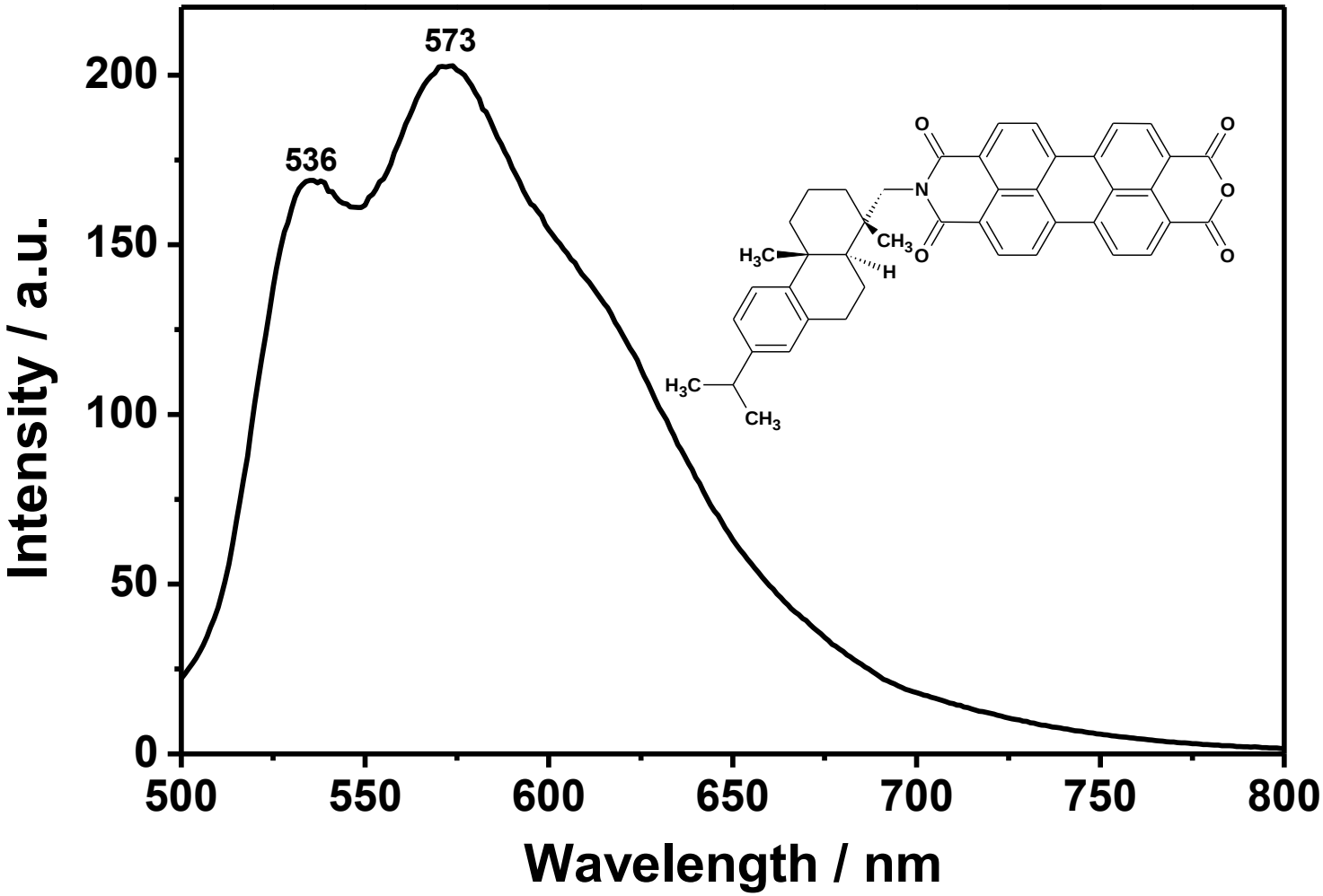

Figure 4.16: Emission Spectrum of ABPMI in CHL

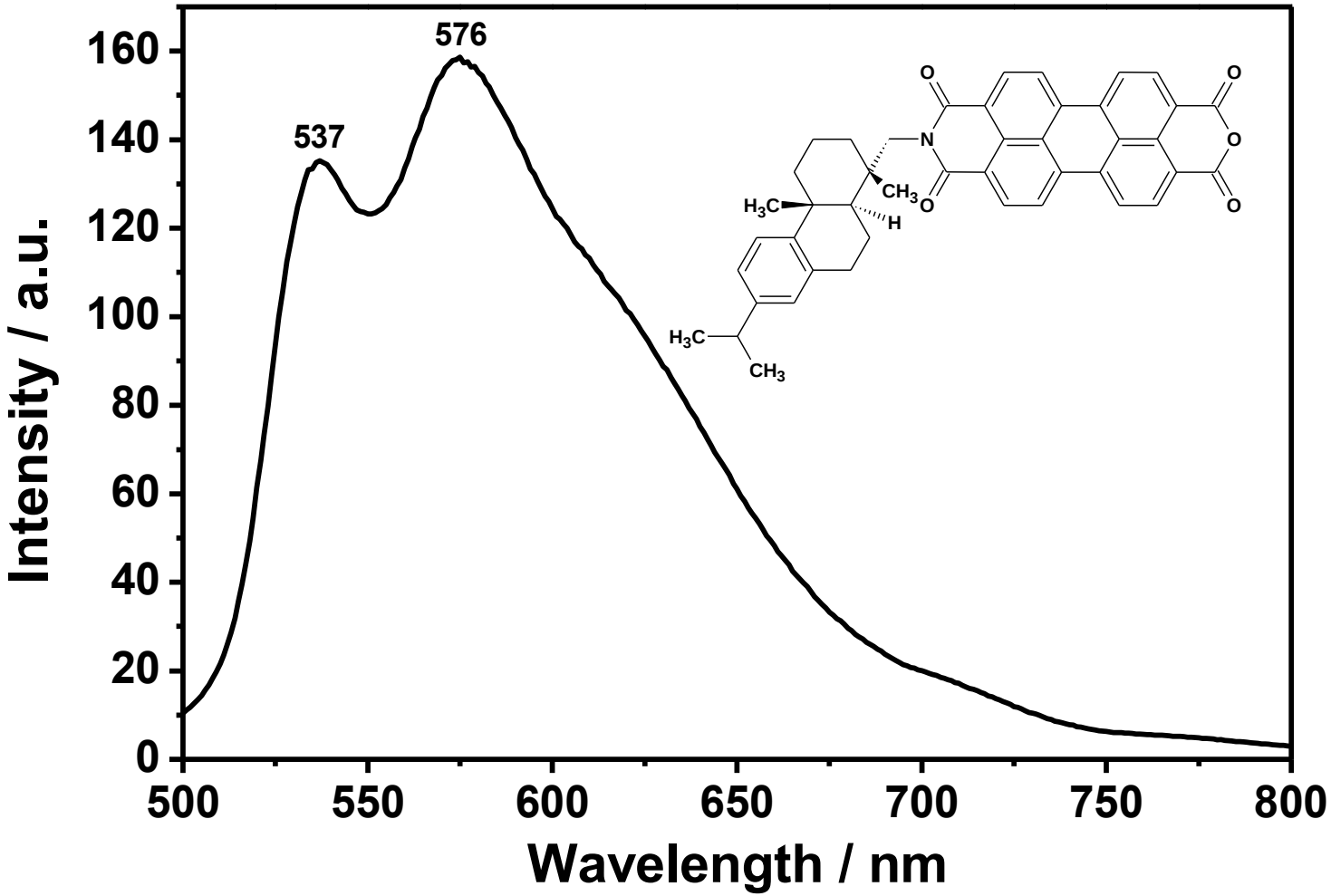

Figure 4.17: Emission Spectrum of ABPMI in DMF

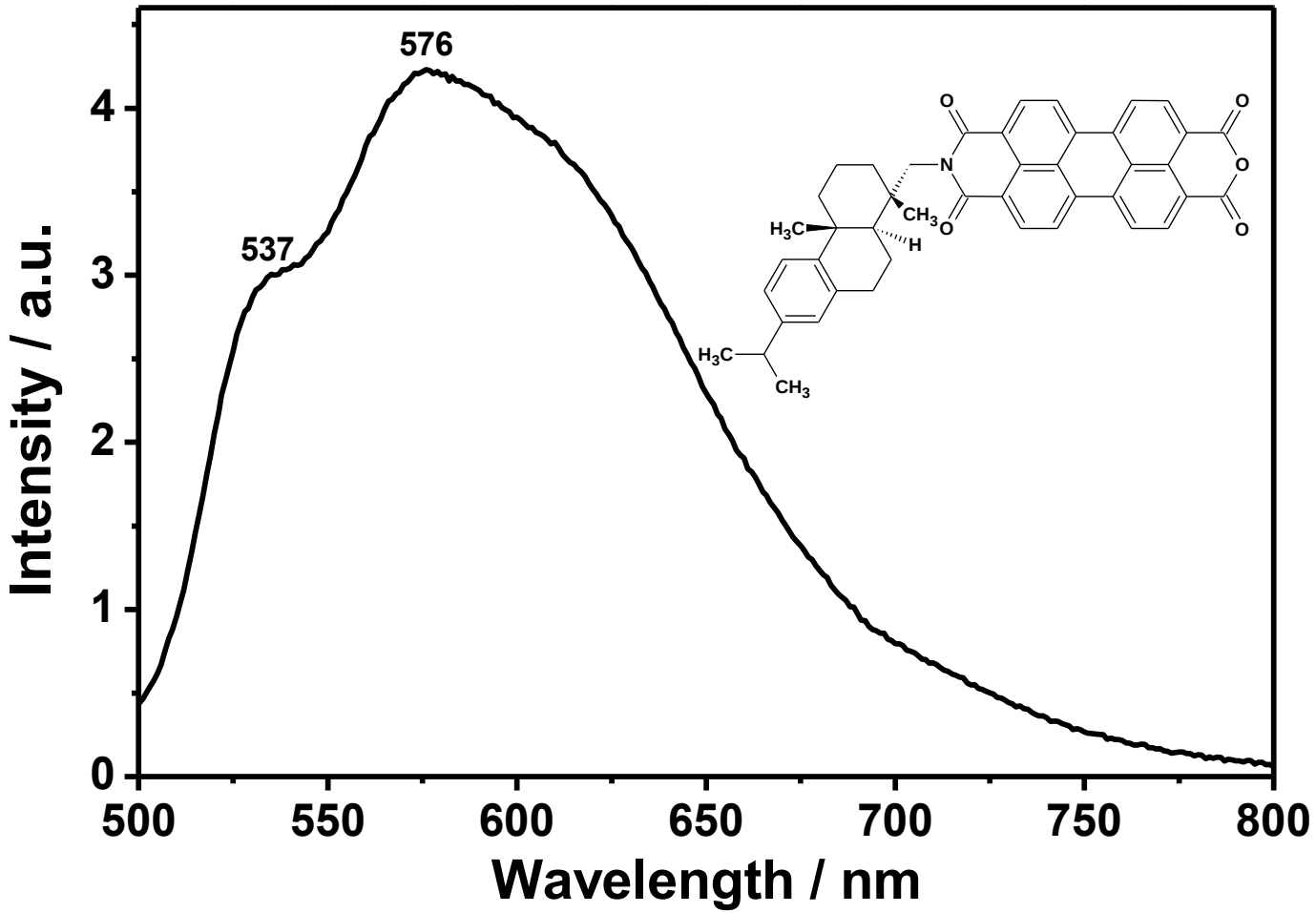

Figure 4.18: Emission Spectrum of ABPMI in MeOH

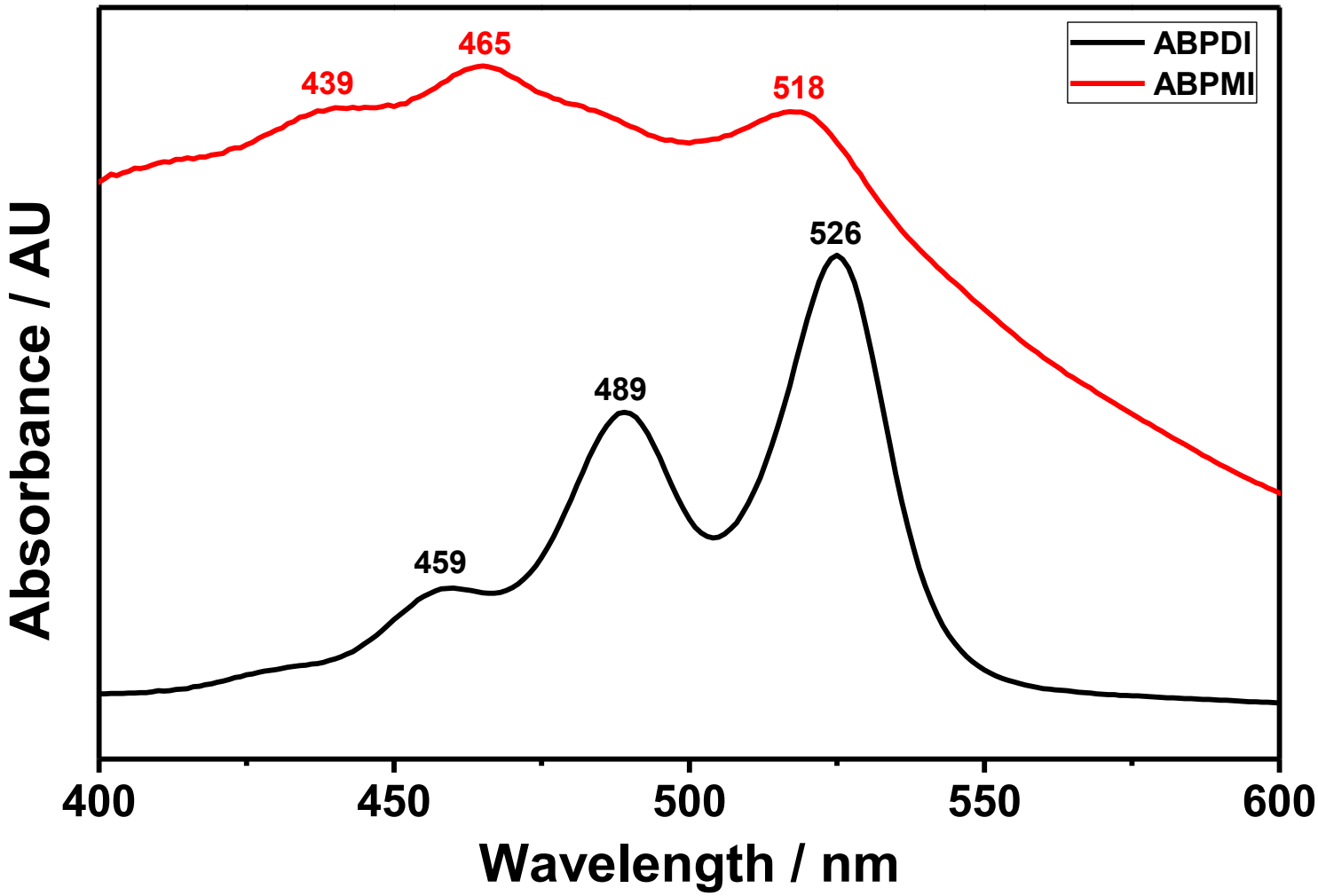

Figure 4.19: UV-vis overlap of ABPDI and ABPMI in DMF

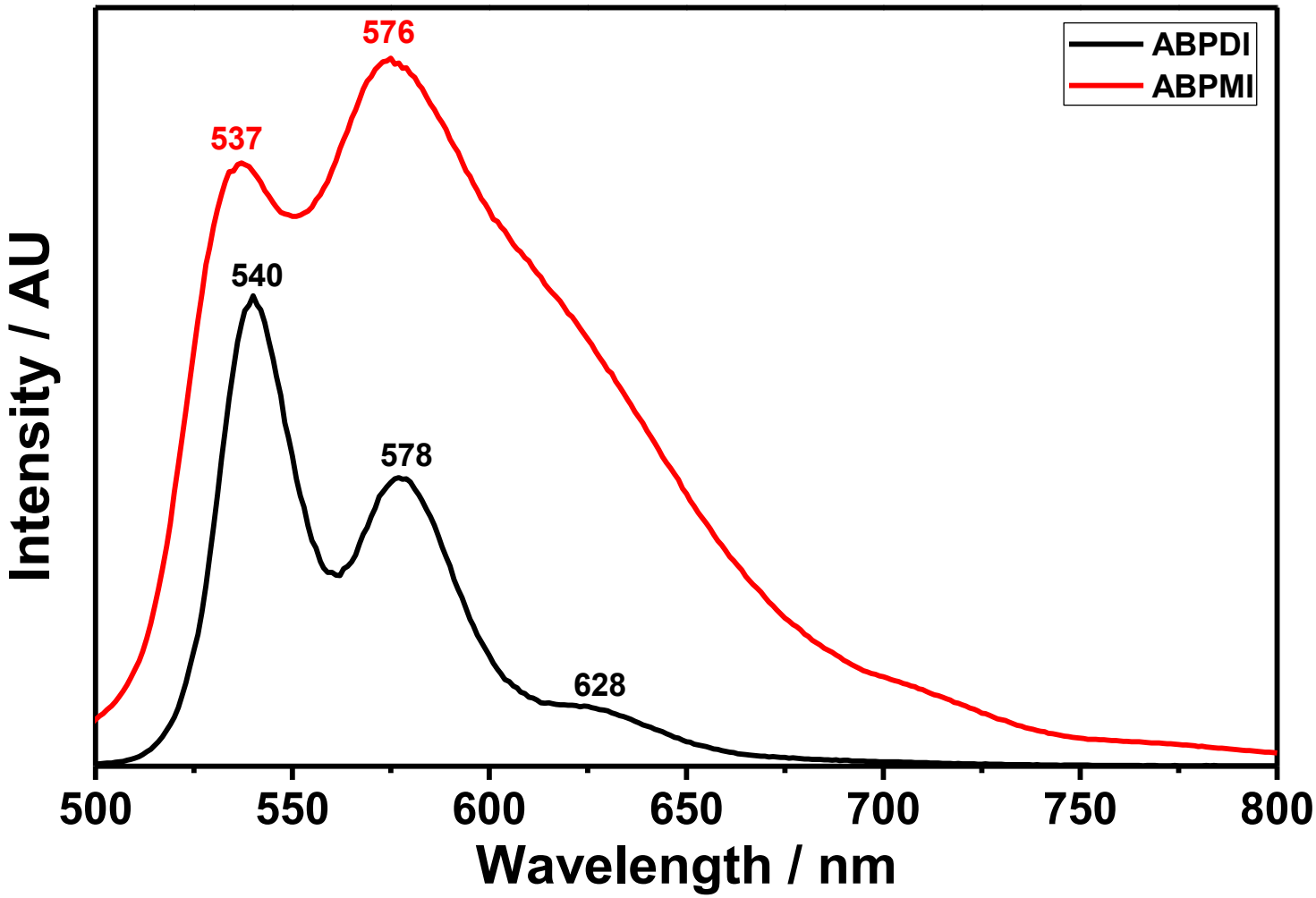

Figure 4.20: Emission overlap of ABPDI and ABPMI in DMF

Chapter 5

RESULT AND DISCUSSION

5.1 Syntheses of the Designed Perylene imide Derivatives

A symmetrical perylene dye was synthesized according to procedures [36]. The synthesis methods were consisting of two steps. In general,At the first step, Synthesis of N-N'-di (1-dehydroabietyl) perylene 3, 4, 9, 10-bis (Dicarboxymide) was done in a successful way. It was obtained through the condensation reaction of amine at the end part of perylene structure. At the second step, N-(1-dehydroabietyl) - 3, 4, 9, 10-perylenetetracarboxylic-3, 4-anhydride-9, 10-imide was synthesized. The characterizations of the final product were done by FTIR spectra. It was taken in the solid state by applying of KBr pallets (Figure 4.4-4.5).

5.2 Structure Confirmation of Synthesized Perylene imide Derivatives

The Table 5.1 illustrates the solubility of ABPDI and ABPMI in three different organic solvents. Briefly, It is clear that the solubility of ABPDI is more than that of corresponding PMI (ABPMI).

Table 5.1: Solubility of ABPDI and ABPMI in different solvent

Compound	ABPDI		ABPMI	
	Cold	Hot	Cold	Hot
CHl	Completely soluble Color: red-orange (+ +)	Completely soluble Color: red-orange (+ +)	Partially soluble Color: red (- +)	Partially soluble Color: red (- +)
DMF	Completely soluble Color: red-orange (+ +)	Completely soluble Color: red-orange (+ +)	Partially soluble Color: red (- +)	Partially soluble Color: red (- +)
MeOH	Partially soluble Color: red (- +)	Partially soluble Color: red (- +)	Partially soluble Color: red (- +)	Partially soluble Color: red (- +)

The solubility property depends on, symmetry and strength of chemical bonds which has effect on inter-molecular interactions. The important factor affecting the solubility, is π-π stacking interactions of compound with solvents. The secondary adjacent carbon atom to the nitrogen impacts on the other substitutions. This factor leads to rotation of the molecular plane of the substitution to the out direction. Thus, it will ultimately leads to inhibition of π-π interaction of the compounds and gives greater solubility.

5.3 IR Spectra

According to IR spectrum of Figure 4.5, the aliphatic —CH Stretch at 2950 cm^{-1}, 2930 $cm^{-1}$and 2867 cm^{-1}, (imide peaks) C=O stretch at 1698 cm^{-1} and 1655 cm^{-1}, aromatic —C=C stretch at 1593$cm^{-1}$and 1507 cm^{-1}, C—N stretch at 1334 cm^{-1}, aromatic C—H bend at 810 cm^{-1} and 754 cm^{-1} will be appear.

With respect to IR spectrum in Figure 4.6, the aliphatic —CH Stretch at 2959 cm^{-1}, aliphatic —CH stretch at 2927 cm^{-1} and 2869 cm^{-1} will be observed. The anhydride C=O stretch at 1775 cm^{-1} shows one peak that have been overlapped with another anhydride peak. Finally, it shows a single peak. The other peak at 1707 cm^{-1} belongs to imide C=O stretch. Conjugated C=C stretch at 1656 cm^{-1} and 1594 cm^{-1}. C—N stretch at 1382 cm^{-1}, C—O—C stretch at 1288 cm^{-1}, C—H bending for aromatic gives two peaks at 820 cm^{-1} and 806 cm^{-1}.

5.4 Optical Properties

The optical properties of ABPDI and synthesized ABPMI are investigated via UV-vis absorption spectrometer and emission spectrometer. The data achieved from absorption and emiision spectra leads to calculation of diverse optical parameters. They are tabulated in Table 4.1- 4.13.

The absorbance phenomenon depends on the polarity of the solvent. The absorption spectra of ABPDI in CHL, DMF and MeOH have been shown in Figure 4.7- 4.9.

Figure 4.7 indicates the absoption spectra of ABPDI in CHL (nonpolar solvent). There are three kinds of characteristic peaks at 459 nm, 490 nm and 526 nm related to $0 \rightarrow 0$, $0 \rightarrow 1$, $0 \rightarrow 2$ electronic transiotions, respectively. These are created due to π-π^* stacking interactions of perylene chromophore. The molar absorptivity values of ABPDI in three different types of solvents have been given in Table 4.1. The highest ε_{max} was obtained in CHL (ε_{max}= 130000 $L.mol^{-1}.cm^{-1}$). It refers to strong absorption in the visible region for ABPDI. It's because of $0 \rightarrow 0$ transition.

Figure 4.8 illustrates ABPDI in a polar aprotic solvent like DMF. The absorption spectra shows three characteristic peaks at 459 nm, 489 nm and 525 nm,

respectively. They refers to $\pi \rightarrow \pi^*$ transitions ($0 \rightarrow 0$, $0 \rightarrow 1$, $0 \rightarrow 2$) from ground state to excited state.

ABPDI exhibits three peaks in MeOH (polar protic solvent) (Figure 4.9) which are at 490 nm, 521 nm and at 574 nm, respectively. The peak at 574 belongs to aggregation. The peaks at 490 and 521 nm refer to $\pi \rightarrow \pi^*$ electronic transitions ($0 \rightarrow 1$, $0 \rightarrow 0$).

The absorption spectra of ABPMI in CHL, DMF and MeOH have been shown in Figure 4.13- 4.15.

There are three kinds of peaks at 439 nm, 469 nm and 517 nm in nonpolar solvent CHL (Figure 4.13). These have arisen from π-π stacking interaction of perylene chromohore. They are typical absorption peaks belong to classic perylenes. In other words, three peaks are because of the $\pi \rightarrow \pi^*$ electronic transitions from the ground state to the excited states. ($0 \rightarrow 0$, $0 \rightarrow 1$ and $0 \rightarrow 2$ transitions).

Figure 4.14 shows the absorption bands for ABPMI in DMF. There are three peaks at 439 nm, 465 nm and 518 nm, respectively. They refers to $\pi \rightarrow \pi^*$ transitions ($0 \rightarrow 0$, $0 \rightarrow 1$, $0 \rightarrow 2$) from ground state to excited state. In Table 4.1, the molar absorptivity values of ABPMI in three kinds of organic solvent have been shown. The highest ε_{max} was obtained in DMF (ε_{max}= 170000 $L.mol^{-1}.cm^{-1}$). It refesr to strong absorption in the visible region for ABPDI. It's because of $0 \rightarrow 0$ transition.

ABPMI has three characteristic peaks in MeOH (polar parotic solvent) (Figure 4.15). They can be seen at 439 nm, 471 nm and 511 nm, respectively. They refer to $\pi \rightarrow \pi^*$ electronic transitions.

Figure 4.19 illustrates a comparision between the absorption spectrum of ABPDI and ABPMI in DMF. The absorption bands are much broder in ABPMI. It could be due to the aggregation of ABPMI with solvents of moderate solubility.

The emission spectrum of ABPDI in CHL, DMF and MeOH have been shown in Figure 4.10- 4.12.

Figure 4.10 shows emission spectrum of ABPDI in CHL as nonpolar solvent. There are three kinds of characteristic peaks at 538 nm, 576 nm and 624. These are due to, π-π stacking interaction of conjugated perylene chromohore. In other words, three peaks are because of the $\pi \rightarrow \pi^*$ electronic transitions ($0 \rightarrow 0$, $0 \rightarrow 1$ and $0 \rightarrow 2$ transitions).

The emission spectrum of ABPDI in DMF shows three characteristic peaks at 540 nm, 578 nm and 626 nm (Figure 4.11). They refer to $\pi \rightarrow \pi^*$ transitions ($0 \rightarrow 0$, $0 \rightarrow 1$, $0 \rightarrow 2$ of perylene chromophore.

ABPDI exhibits two bands in MeOH (polar parotic solvent) (Figure 4.12). They can be seen at 537 nm and 577 nm. They refers to $\pi \rightarrow \pi^*$ electronic transitions ($0 \rightarrow 0$ and $0 \rightarrow 1$electronic transitions).

The emission spectra of ABPMI in CHL, DMF and MeOH have been shown in Figure 4.16- 4.18.

Figure 4.16 shows emission of ABPDI in CHL as nonpolar solvent. There are two kinds of characteristic peaks at 536 nm and 573 nm . These are due to, π-π stacking interaction of conjugated perylene chromohore. In other words, two peaks are because of the $\pi \rightarrow \pi^*$electronic transitions ($0 \rightarrow 0$, $0 \rightarrow 1$ transitions).

Figure 4.17 illustrates ABPDI in a polar aprotic solvent like DMF. The emission bands of ABPMI in DMF shows two peaks at 537 nm and 576 nm. They refers to $\pi \rightarrow \pi^*$ transitions ($0 \rightarrow 0$, $0 \rightarrow 1$) of perylene chromophore.

ABPMI exhibits two broad emission bands in MeOH (polar parotic solvent) (Figure 4.18). They can be seen at 537 nm and 576 nm. They refers to $\pi \rightarrow \pi^*$ electronic transitions.

Figure 4.20 shows a comparision between the emission spectrum of ABPDI and ABPMI in DMF. The emission bands are broder in ABPMI than corresponding ABPDI. It is due to formation of the excimer- like emission complex.

Chapter 6

CONCLUSION

In the reported project focused on the design and synthesis of a novel perylene derivative, N-(1-dehydroabietyl) - 3, 4, 9, 10-perylenetetracarboxylic-3, 4-anhydride-9, 10-imide (ABPMI), from previuos synthesized N-N'-di (1-dehydroabietyl) perylene 3, 4, 9, 10-bis (Dicarboxymide) (ABPDI). The chiral structures were synthesized due to their considerable optical features beside their unique stabilities. Both compounds were investigated by FTIR to explain their structure by determination of main functional groups, thin layer chromatography (TLC) to obtain their R_f value and UV-vis and fluorescence spectrums to describe their optical properties.

The thin layer chromatography characterization of ABPDI and ABPMI shows R_f value of 25.0% and zero, respectively. While, ABPDI moved through the silica plate. ABPMI did not. According to that, ABPMI was more polar than ABPDI.

The FTIR spectra of two coumpounds show clear differences in the structure of ABPDI and ABPMI. The spectra indicated characteristic peaks related to their functional groups. ABPDI shows two distinct peaks at 1698 and 1655 cm^{-1} for imide groups while, ABPMI illustrates two peaks for imide and anhydride groups (1707 and 1656 cm^{-1}).

The solubility of both compounds was tested in nonpolar, polar aprotic and polar protic sovents such as CHL, DMF and MeOH, respectively. ABPDI was soluble in all three organic solvents whereas, the solubility of ABPMI was moderate in mentioned solvents.

The absorption spectra of ABPDI and ABPMI were investigated in CHL (nonpolar solvent), DMF (polar aprotic solvent) and MeOH (polar protic solvent). They show three distictive peaks for electronic transition of perylene chromophoric compounds. Absorption spectrum of ABPMI shows broadening due to aggregation. The molar extinction coefficient (ε_{max}) of ABPMI(113700 $L.mol^{-1}.cm^{-1}$) is higher than ABPDI (115000 $L.mol^{-1}.cm^{-1}$), in DMF.

The emission spectra of both compounds were studied in three organic solvent (CHL, DMF, MeOH). They indicate two distinctive peaks belonging to electronic transitions of perylene chromophore. Emission spectrum of ABPMI in DMF shows excimer-like emission complex. The flourescence quantum yield of ABPDI was 1. It calculated as for 0.45 for ABPMI in DMF.

Future work

1. Opening of anhydride group to obtain dicarboxylic groups to enhance the solubility.
2. Studying on interactions of ABPMI with DNA in different pH media
3. Studying on stability of the complex that will be generated between DNA and ABPMI

REFERENCES

[1] Heek T., Wurthner F & Haag R. (2013). Synthesis and Optical Properties of Water-Soluble Polyglycerol-Dendroinized Rylene Bisimide Dyes. *Journal of Chemistry*. 19 (13) 10911-10921

[2] Pignataro, B. (2010). Ideas in Chemistry ad Molecular science: Advanced in synthetic chemistry . *Journal of John Wiley&sons.*ISBN:978_3_527_32543_6

[3] Incles C.M., Schultes C.M & Neidle S. (2003) Telomerase Inhibitors In Cancer Theapy: Current Status and Future Directions. *Journal of Current Opinion in Investigational Drugs.* 4 (6) 675-685

[4] Cunningham A.P., Love W.K & Tollefsbol TO.(2006).Telomerase Inhibition in Cancer Therapeutics: Molecular-Based Approaches. *Journal of Current Medicinal Chemistry*. 13 (24) 2875-2888

[5] Thomas D.W. (1999) Cellular Senescence and Cancer. *Journal of Pathology.* 187 (1) 100-111

[6] Russell P. (2001). I Genetics. A Molecular approach. New York: *Benjamin Cumming.* ISBN 0-8053-4553-1

[7] Greider C.,Blackburn E. (1958). Identification of a Specific Telomere Terminal Transferase Activity in Tetrahymena Extracts. *Journal of Cell.*43 (1-2) 405-413

[8] Burge S & Neidle S. (2006). Quadruplex DNA: Sequence, Topology and Structure. Journal of Nucleic Acid Reserch. 34 (19) 5402-5415

[9] Parkinson G & Neidle S.(2002). Crystal Structure of Parallel Quadruplexes from Human Telomeric. *Jornal of Nature.* 417 (6891) 876-880

[10] Ruden M & Puri,N.(2013). Novel Anticancer Therapeutics Targeting Telomerase. *Journal of Cancer Treatment Reviwe.* 39 (5) 444-456

[11] Chaires, J, B. (1998). DNA Drug Interaction. *Journal of Current Opinion in Structural Biology.* 8 (3) 314-320

[12] Perun,J,Th Propst,C,L .(1992).Nucleic Acid Targeted Drug Design.New york.*Marcel Dekker.* ISBN 0-8247-8662-9

[13] Olaussen, K, A & Soria, C, J. (2006). Telomere and Telomerase as Targets for Anti-cancer Drug Development. *Journal of Oncology Hematology.* 57 (3) 191-214

[14] Csagrande, V & Lachettini, S. (2011). N-Cyclic Bay-substituted Perylene G-quadruplex Ligands Have Selective Anti-proliferative Effects on Cancer Cells and Induce Telomere Damage. *Journal of Medicinal Chemistry* . 54 (5)1140-1156

[15] Leudtke, N, M. (2009). Targeting G-quadruplex DNA with small molecules. *Journal of Chimia.* 63 (3) 134-169

[16] Semenove,V, V & Domracheve, G, A. (2011). Reaction of Perylene Tetracarboxylic Dianhydride with 3-amino propyltriethoxysilane and Hexamethyldisilazane. *Russian Journal of General Chemistry.* 81 (7) 1496-1506.

[17] Wu,J & Zhu,L .(2011). N-Annulated Perylene Dyes with Adjustable Photophysical Properties. *Journal of Tetrahedron.* 52 (48) 6411-6414

[18] Hermmann A & Mulen K. (2006). From Industrial Colorants to Single Photon Sources and Biolables: The Fascination and Function of Reylene Dyes. *Jornal of Chemistry Letters.* 35 (9), 978-985

[20] Icil, H, Ozser, M.E & Makhynya, Y,A. (2004). Electron Transfer-Initiated Cascade Cyclizations of Terpenoid Polyalkenes in Low-Polarity Solvent : One-Step Synthesized of Mono- and Polycyclic Terpenoids With Various Functionalities. *European Journal of Organic Chemistry.* 3686-3692

[21] Icil, H & Ozdal, D. (2013). Synthesis of a Novel Flourscent Amphilic Chitosan Biopolymer : Photophysical and Electrochemical Behavior. *Journal of Dye and Pigments.* 12 (11) 1927-1938

[22] Ozer, E, Mustafa & Icil, H. (2013). New Naphthalene Polyimide with Unusual Molar Absorption Coefficient and Excited State Properties: Synthesis, Photopysics and Electrochemistry. *Jornal of Luminescence. 143, 542-550*

[23] Refiker, H & Icil,H. (2011). Amphilic and Chiral Unsymmetrical Perylene Dye for Solid-state Dye-sensitized Solar Cells. *Turkish Jornal of Chemistry. 35 (6) 847-859.*

[24] Bodapati, J, B & Icil, H. (2011). A New Tunable Light Emitting and Pi-stacked Hexa-ethyeneglycol Naphthalene-bisimide Oligomer: Synthesis, Photophysics and Electrochemical Properties. *Journal of photochemistry.photobiological Sci. 10 3393-3397*

[25] Asir, S & Icil, H. (2010). Efficient Synthesis of New Unsymmetrically Substituted Chiral Naphthalene and Perylene Diimides: Their Photophysical, Electrochemical, Chiroptical and Intramolecular Charge Transfer Properties. *Journal of Dyes and Pigments. 84 1-13*

[26] Amiralaei,S & Icil, H. (2008). Chiral Substituent Containing Perylene Monoanhydride Monoimide and Diimide: Synthesis, Photophysics and Electrochemistry from Dilute Solution to Solid State. *Journal of photochemistry photobiological Sci.* 7 936-947

[27] Bodapati, J, B & Icil, H. (2008). New Soluble Self Organized Polyimide Containing Perylene and Hexa (ethylene glycol) Moieties: Synthesis, Characterization, Photophysical and Electrochemical Properties. *Journal of Dyes and Pigments.* 79 224-335

[28] Yuney, K & *Icil*, H.(2007). Synthesis, Photochemical, Photophysical Properties of Naphthalene-1,4,5,8,tetracarboxylicacids-bis-(N,N-bis-

((2,2,4(2,4,4)trimethylpolyimide) andPoly(N,N-bis-(2,2,4,(2,4,4)-trimethyl-6-aminohexyl)3,4,9,10 Perylenetetracarboximide). . *Eouropean polymer Jornal.* 43 2308-2320

[29] Pasaogullari, N & Icil, H. (2006).Symmetrical and Unsymmetrical Perylene Diimides: Their Synthesis, Photophysical and Electrochemical Properties. *Journal of Dyes and Pigm.*69 118-127

[30] Kern,J.T & Kerwine,S.M.(2002). The Aggregation and G-quadruplex DNA Selectivity of Charged 3,4,9,10_Perylene Tetracarboxylic Acid Diimides. *Journal of Bioorg&Med Chem.* 12 (23) 3395-3398

[31] Yang, L & Chen, H. (2008). Synthesis, Electrochemical, and Spectroscopic Properties of Soluble perylene Monomide Diester. *Journal of tetrahedron.* 64 (22) 5404-5409

[32] Xue,C & Jin,S. (2009). Perylene Mono Anhydride Diester: A Varsetile Intermediate for the Synthesis of Unsymmetrically Substituted Perylene Tetracarboxylic Derivatives. *Journal of Tetrahedron letter.* 50 (8) 853-856

[33] Wang,R & Sun,Zh. (2013).Facile Synthesis and Controllable Bromination of Asymmetrical Intermediates for Perylene monoanhydrie/Monoimide Diester. *Journal of Dyes and Pigm* .98 (3) *450-458*

[34] Abdelsayed,V. & El-Shall S. (2009). Microvave Synthesis of Bimetallic Nanoalloys and CO Oxidation on Ceria-Supported Nanoalloys. Jornal of Chemical Material 21 (13) 2825-2834

[35] Perrin, D.D & Armarego,W.L.F. (1980). Purification of Lobratory Chemicals.2th edition. 249-251 and 321-350

[36] Icil, H & Sayil, C. (1998). Synthesis and Properties of a New Photostable Soluble Perylene Dye : N-N′-di-(1-dehydroabietyl) Perylene -3, 4, 9, 10-bis (dicarboximide). *Jornal of Spectroscopy Letter. 31(8) 1643-1647*

[37] Abdelsayed,V.& El-Shall S. (2009). Microvave Synthesis of Bimetallic Nanoalloys and CO Oxidation on Ceria-Supported Nanoalloys. Jornal of Chemical Material 21 (13) 2825-2834

[38] Icil, H & Icil, S. (1996). Athermal and photostable refrence probe for Q_f measurements: Chloroform Soluble Perylene 3, 4, 9, 10-tetracarboxylic Acid-bis-N,N′-dodecyldiimide. *Jornal of Spectroscopic letter.* 29 (7) 1253-1257

[39] Turro,N,J. (1967). Molecular photochemistry, W.A. Benjamin, Inc. New York.